

PREPARATION OF CELLULOSE MICRO- AND NANO FIBERS FROM BAGASSE  
THROUGH DEEP EUTECTIC SOLVENT SYSTEMS



A Thesis Submitted in Partial Fulfillment of the Requirements  
for the Degree of Master of Science in Petrochemistry and Polymer Science

Field of Study of Petrochemistry and Polymer Science

FACULTY OF SCIENCE

Chulalongkorn University

Academic Year 2022

Copyright of Chulalongkorn University

การเตรียมเส้นใยเซลลูโลสระดับไมโครและนาโนจากชานอ้อยด้วยระบบตัวทำละลายยูเทคติก



วิทยานิพนธ์นี้เป็นส่วนหนึ่งของการศึกษาตามหลักสูตรปริญญาวิทยาศาสตรมหาบัณฑิต สาขาวิชาปิโตรเคมีและวิทยาศาสตร์พอลิเมอร์ สาขาวิชาปิโตรเคมีและวิทยาศาสตร์พอลิเมอร์

คณะวิทยาศาสตร์ จุฬาลงกรณ์มหาวิทยาลัย

ปีการศึกษา 2565

ลิขสิทธิ์ของจุฬาลงกรณ์มหาวิทยาลัย

Thesis Title PREPARATION OF CELLULOSE MICRO- AND NANO FIBERS  
FROM BAGASSE THROUGH DEEP EUTECTIC SOLVENT  
SYSTEMS

By Mr. Worapoj Phuckpetch

Field of Study Petrochemistry and Polymer Science

Thesis Advisor Associate Professor SURACHAI PORNPAAKAKUL, Ph.D.

---

Accepted by the FACULTY OF SCIENCE, Chulalongkorn University in Partial Fulfillment of  
the Requirement for the Master of Science

THESIS COMMITTEE

..... Dean of the FACULTY OF SCIENCE  
(Professor POLKIT SANGVANICH, Ph.D.)

..... Chairman  
(Professor PRANUT POTIYARAJ, Ph.D.)

..... Thesis Advisor  
(Associate Professor SURACHAI PORNPAAKAKUL, Ph.D.)

..... Examiner  
(Associate Professor SIRILUX POOMPRADUB, Ph.D.)

..... External Examiner  
(Professor Sophon Roengsumran, Ph.D.)

วรพจน์ พักเพ็ชร : การเตรียมเส้นใยเซลลูโลสระดับไมโครและนาโนจากชานอ้อยด้วยระบบตัวทำละลายยูเทคติก. ( PREPARATION OF CELLULOSE MICRO- AND NANO FIBERS FROM BAGASSE THROUGH DEEP EUTECTIC SOLVENT SYSTEMS) อ.ที่ปรึกษาหลัก : รศ. ดร. สุรัชชัย พรภาคกุล

งานวิจัยนี้เป็นการเตรียมเส้นใยเซลลูโลสระดับไมโครและนาโนจากชานอ้อยด้วยกระบวนการที่เป็นมิตรต่อสิ่งแวดล้อม โดยการปรับปรุงเส้นใยชานอ้อยที่ผ่านกระบวนการฟอกขาวแล้วด้วยตัวทำละลายยูเทคติกระหว่าง ซิงค์คลอไรด์และกรดแลคติก  $ZnCl_2$ -LA DES จากการทดลองปรับปรุงเส้นใยชานอ้อยด้วยตัวทำละลายยูเทคติก พบว่าตัวทำละลายยูเทคติกทำหน้าที่หลายอย่างในกระบวนการปรับปรุงเส้นใย เช่นการเป็นตัวทำละลาย ตัวเร่งปฏิกิริยา และสารตั้งต้นเอง ภายใต้สภาวะที่เหมาะสมเราปรับปรุงเส้นใยชานอ้อย 6.25% โดยมวลในตัวทำละลายยูเทคติก และทำการแยกเส้นใยด้วยคลื่นความถี่สูงจนได้เส้นใยที่มีความยาว 230-270 นาโนเมตร และความกว้าง 15-16 นาโนเมตร มีค่าเปอร์เซ็นต์ผลึกที่ 62.2% และเส้นใยที่ได้มีหมู่ฟังก์ชันเป็นกรดแลคติกบนพื้นผิว ร้อยละผลได้ที่ได้รับมีค่ามากกว่า 90% ตัวทำละลายยูเทคติกที่ผ่านการใช้งานแล้วสามารถนำกลับมาใช้ใหม่ได้หลังผ่านกระบวนการทำความสะอาด โดยสามารถนำกลับมาใช้ซ้ำได้มากกว่า 5 ครั้ง และตัวทำละลายที่ผ่านการใช้งานยังสามารถนำมาแยกองค์ประกอบของสังกะสี สารประกอบสังกะสีที่แยกได้สามารถนำไปใช้เป็นสารตั้งต้นในการผลิตซิงค์คลอไรด์เพื่อเตรียมตัวทำละลายยูเทคติกใหม่ได้อีก ตัวทำละลายที่เหลือหลังจากกระบวนการแยกสังกะสีไปแล้วมีความปลอดภัยสูงและสามารถกำจัดทิ้งได้โดยมีผลกระทบต่อสิ่งแวดล้อมต่ำ



สาขาวิชา	ปิโตรเคมีและวิทยาศาสตร์พอลิเมอร์	ลายมือชื่อนิสิต .....
ปีการศึกษา	2565	ลายมือชื่อ อ.ที่ปรึกษาหลัก .....

# # 6172051623 : MAJOR PETROCHEMISTRY AND POLYMER SCIENCE

KEYWORD:

Worapoj Phuckpetch : PREPARATION OF CELLULOSE MICRO- AND NANO FIBERS FROM BAGASSE THROUGH DEEP EUTECTIC SOLVENT SYSTEMS. Advisor: Assoc. Prof. SURACHAI PORNPAKAKUL, Ph.D.

This study aimed to prepare the cellulose micro- and nanofibers (CMNFs) using green chemistry viewpoint. The CMNFs were fabricated from sugarcane bagasse (SCB) pulp through treatment with zinc chloride ( $\text{ZnCl}_2$ ) - lactic acid (LA) in deep eutectic solvent ( $\text{ZnCl}_2$ -LA DES) followed by short time ultrasonication of the DES-treated fibers in water. Under the optimum condition, the SCB pulp at high solid loading of 6.25% was treated with  $\text{ZnCl}_2$ -LA DES. Lactate functionalized CMNFs with 230-270 nm length and 15-16 nm width were resulted in more than 90% yield and up to 62.2% crystallinity. The results showed that  $\text{ZnCl}_2$ -LA DES was a multi-functional green solvent by acting as solvent, catalyst, and substrate. Also, the  $\text{ZnCl}_2$ -LA DES could be reused for more than 5 times with slight decrease of performance. Zinc ion could be separated from  $\text{ZnCl}_2$ -LA DES after used with simple precipitate method and the remained solution mainly contained of saccharides and lactic acid which can be disposed safely after neutralization or used as substrate for fermentation. Overall,  $\text{ZnCl}_2$ -LA DES treatment followed by ultrasonication had proven to be effective and environmentally friendly procedure for preparation lactate functionalized CMNFs from SCB pulp.

จุฬาลงกรณ์มหาวิทยาลัย  
CHULALONGKORN UNIVERSITY

Field of Study:	Petrochemistry and Polymer Science	Student's Signature .....
Academic Year:	2022	Advisor's Signature .....

## ACKNOWLEDGEMENTS

I am especially grateful to my advisor, Associate Professor Dr. Surachai Pornpakakul, for excellent suggestions and valuable comments in every part of my research. I would like to thank my advisor for his kindness for support and encouragement to give me good opportunities during this research.

Moreover, I would like to thank Professor Dr. Pranut Potiyaraj, for serving as the chairman, Associate Professor Dr. Sirilux Poompradub and Professor Dr. Sophon Roengsumran for serving as examiner of my thesis committee, respectively, for their valuable suggestions and comments.

Additionally, I am enormously grateful to the faculty members of the Petrochemical and Polymer Science Program, at Chulalongkorn University for giving me knowledge. I would like to thank all those people and the members of my laboratory who provide happiness and support for me to complete this thesis.

Finally, I am also thankful to my family and my nice friends for their assistance and encouragement throughout my research period.

Worapoj Phuckpetch

## TABLE OF CONTENTS

	Page
.....	iii
ABSTRACT (THAI).....	iii
.....	iv
ABSTRACT (ENGLISH).....	iv
ACKNOWLEDGEMENTS.....	v
TABLE OF CONTENTS.....	vi
LIST OF TABLES.....	x
List of figures.....	xi
CHAPTER I INTRODUCTION.....	1
1.1. The Statement of Problem.....	1
CHAPTER II THEORY AND LITERATURE REVIEWS.....	4
2.1. Sugarcane bagasse.....	4
2.2. Lignocellulose.....	4
2.2.1. Cellulose.....	5
2.2.1.1. Source.....	5
2.2.1.2. Existence of Cellulose.....	6
2.2.1.3. Crystalline.....	7
2.2.1.4. H-bonding.....	8
2.2.2. Hemicellulose.....	9
2.2.3. Lignin.....	9
2.3. Nanocellulose.....	10

2.3.1.	Cellulose microfibers .....	11
2.3.2.	Celluloses nanofibers .....	11
2.3.3.	Bacterial cellulose nanofibers.....	12
2.3.4.	Cellulose nanocrystals .....	13
2.3.5.	Spherical cellulose nanoparticles.....	13
2.4.	Nanocellulose fabrications .....	14
2.4.1.	Top-down approaches .....	14
2.4.1.1.	Mechanical disintegration .....	14
2.4.1.1.1.	High-pressure homogenization.....	14
2.4.1.1.2.	Microfluidization.....	15
2.4.1.1.3.	Grinding method.....	16
2.4.1.1.4.	Cryocrushing.....	16
2.4.1.1.5.	High-intensity ultrasonication .....	16
2.4.1.1.6.	Aqueous counter collision .....	17
2.4.1.1.7.	Ball milling collision.....	18
2.4.1.2.	Chemical treatment.....	18
2.4.1.2.1.	Acid hydrolysis.....	18
2.4.1.2.2.	Hydrolysis with solid acid.....	19
2.4.1.2.3.	Ionic liquid treatment .....	19
2.4.1.2.4.	TEMPO oxidation.....	20
2.4.1.3.	Enzymatic pretreatment .....	20
2.4.2.	Bottom-up approaches .....	21
2.4.2.1.	Electrospinning.....	21
2.4.2.2.	Bacterial biosynthesis .....	22



2.5. Deep eutectic solvents .....	22
2.6. Literatures survey.....	23
CHAPTER III EXPERIMENTAL.....	27
3.1. Materials .....	27
3.1.1. Sugarcane Bagasse .....	27
3.1.2. Chemicals .....	27
3.2. Glassware and equipment .....	27
3.3. Instruments .....	28
3.4. Experimental Procedures .....	28
3.4.1. Preparation of sugarcane bagasse pulp.....	28
3.4.2. Preparation of ZnCl <sub>2</sub> -LA DES.....	28
3.4.3. Fabrication of CMNFs .....	28
3.4.4. Preparation of neat lactic acid pretreated fibers .....	29
3.4.5. Reusing of ZnCl <sub>2</sub> -LA DES.....	29
3.4.6. Recover of Zinc .....	29
3.5. Characterizations.....	30
3.5.1. Polarized light Microscopy .....	30
3.5.2. Fourier transform infrared spectroscopy.....	30
3.5.3. X-Ray diffraction .....	30
3.5.4. Transmission electron microscopy.....	30
3.5.5. <sup>13</sup> C and <sup>1</sup> H nuclear magnetic resonance spectroscopy .....	30
3.5.6. <sup>13</sup> C CP/MAS solid NMR spectroscopy.....	31
3.5.7. Dynamic light scattering.....	31
CHAPTER IV RESULTS AND DISCUSSION .....	32

4.1	Preparation of sugarcane bagasse pulp .....	32
4.2	Preparation of ZnCl <sub>2</sub> -LA DES .....	35
4.2.1.	NMR analysis .....	35
4.3	Preparation of neat lactic acid pretreated fibres .....	37
4.4	Fabrication of CMNFs .....	38
4.2.1.	Morphology of fibres .....	38
4.2.2.	Particles size .....	41
4.2.3.	Characteristics of fibres .....	43
4.2.4.	Mechanism .....	47
4.5	Preparation of CMNF films .....	48
4.6	Reusing of ZnCl <sub>2</sub> -LA DES .....	48
4.2.1.	Reuse of ZnCl <sub>2</sub> -LA DES .....	48
4.2.2.	NMR analysis .....	50
4.7	Recover of zinc .....	52
CHAPTER V CONCLUSION .....		53
5.1.	Conclusion .....	53
REFERENCES .....		54
VITA.....		61

## LIST OF TABLES

	<b>Page</b>
Table 1. Classifications of nanocellulose and synthesis method[43]. .....	10
Table 2. Type of DESs[47].....	23
Table 3. DLS results of CMNFs from different reaction temperatures and times. ....	43
Table 4. CMNF dimensions and CrI from different temperature.....	43
Table 5. CMNF dimensions and CrI from different temperature.....	46
Table 6. Yield and CMNF sizes reply to ZnCl <sub>2</sub> -LA DES reusing times. ....	49

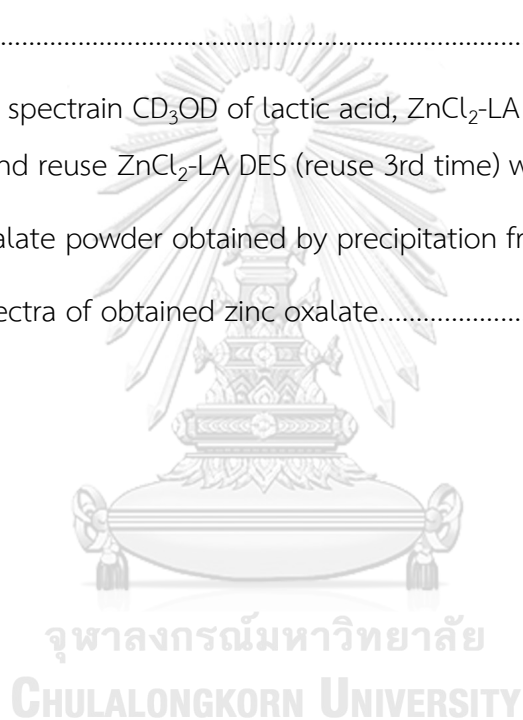


## List of figures

	Page
Figure 1. Thailand's production of sugarcane bagasse (thousand metric tons) [40]. ....	4
Figure 2. Chemical structure of $\beta$ -D-glucose.....	5
Figure 3. Chemical structure of cellulose polymer chain.....	5
Figure 4. Plant cell wall structure [41].....	6
Figure 5. Cellulose crystalline lattice structure [42].....	7
Figure 6. H-bonding between cellulose molecule [43].....	8
Figure 7. Conformation of C6-OH moiety in cellulose chain [43]. ....	8
Figure 8. Hemicellulose's common monomers [44]. ....	9
Figure 9. Scanning electron microscope (SEM) image of cellulose microfibrils[45]. ...	11
Figure 10. SEM image of cellulose nanofiber[45]. ....	12
Figure 11. SEM image of bacterial cellulose nanofiber[45]. ....	12
Figure 12. SEM image of spherical cellulose nanoparticles[45].....	13
Figure 13. Equipment diagram and Mechanism of high-pressure homogenization[45].....	15
Figure 14. Equipment diagram of microfluidization technique[43].....	15
Figure 15. Equipment diagram show how grinding method works[43]. ....	16
Figure 16. Defibrillation of lignocellulose fiber with high-intensity ultrasonication[45]. .....	17
Figure 17. Equipment diagram of aqueous counter collision technique[45].....	17
Figure 18. Diagrams show different type of grinding methods[45].....	18
Figure 19. diagram show dissolution mechanism of cellulose in ILs. ....	19
Figure 20. diagram show mechanism of cellulose oxidation with TEMPO[45]. ....	20

Figure 21. Preparation of cellulose nanofibers with electrospinning method[45].	21
Figure 22. Shows different chemicals using as hydrogen bond acceptor and hydrogen bond donor[47].	23
Figure 23. Raw sugarcane bagasse.	32
Figure 24. FTIR spectra of (a) raw bagasse, (b) DI water washed bagasse, (c) bleached bagasse pulp.	34
Figure 25. Appearance of bleached bagasse pulp.	34
Figure 26. Bleached bagasse pulp under polarized-light microscope.	34
Figure 27. Appearance of ZnCl <sub>2</sub> -LA DES.	35
Figure 28. <sup>1</sup> H NMR spectra of a. lactic acid and b. ZnCl <sub>2</sub> -LA DES in CD <sub>3</sub> OD.	36
Figure 29. <sup>13</sup> C NMR spectra of of a. lactic acid and b. ZnCl <sub>2</sub> -LA DES in CD <sub>3</sub> OD.	36
Figure 30. The visual representation of the bagasse mixture treated with lactic acid after a 120-minute reaction period.	37
Figure 31. PLM image of lactic acid pretreated bagasse fibre after fabrication with ultrasonic homogenizer.	38
Figure 32. PLM images of DES treated SCB pulp swollen in DI water.	39
Figure 33. PLM images of CMNF fibers obtained by treatment of the DES treated SCB in water with ultrasonication for 10 minutes.	41
Figure 34. TEM images of CMNF from different temperatures at: (a) 90 °C, (b) 100 °C, (c) 110 °C, and (d) 120 °C for 120 min.	42
Figure 35. (a) FTIR spectra of bleached SCB pulp and CMNF samples from different temperature, (b) and (c) Cropped FTIR spectra.	44
Figure 36. <sup>13</sup> C solid-state NMR of CMNF obtained from ZnCl <sub>2</sub> -LA DES treated CMNF.	45
Figure 37. XRD results of obtained CMNF.	46

Figure 38. Possible mechanism of cellulose chain cleavage and functionalized in ZnCl <sub>2</sub> -LA DES.....	47
Figure 39. Cellulose films obtained from fibers treated with ZnCl <sub>2</sub> -LA at 110 oC for: (a) 30 minutes and (b) 120 minutes .....	48
Figure 40. Images of used solvent from different temperatures and reaction times.	49
Figure 41. PLM images of CMNF fibers obtained by SCB pretreated with reuse DES...	50
Figure 42. <sup>1</sup> H NMR spectra in CD <sub>3</sub> OD of ZnCl <sub>2</sub> -LA DES ,used ZnCl <sub>2</sub> -LA DES, reuse ZnCl <sub>2</sub> -LA DES.....	51
Figure 43. <sup>1</sup> H NMR spectrain CD <sub>3</sub> OD of lactic acid, ZnCl <sub>2</sub> -LA DES, reuse ZnCl <sub>2</sub> -LA DES (reuse 3rd time), and reuse ZnCl <sub>2</sub> -LA DES (reuse 3rd time) with ZnCl <sub>2</sub> added.....	51
Figure 44. zinc oxalate powder obtained by precipitation from used DES.....	52
Figure 45. XRD spectra of obtained zinc oxalate.....	52



# CHAPTER I

## INTRODUCTION

### 1.1. The Statement of Problem

Sugarcane bagasse, a primary waste in table sugar industrials, was produced approximately 270 kg for every 1000 kilograms of processed sugarcane [1]. The utilizations of this agricultural waste were limited due to high cost of operations and chemicals consumption. The main benefit of bagasse is to produce heat and electricity and use for paper making [1, 2]. Since the bagasse is lignocellulosic biomass containing lignin (20.60%), hemicellulose (21.87%), and cellulose (37.61%) [3], it can be used as a feedstock to produce various high-value biobased chemicals. Among those compositions, cellulose as the largest portion can be used for the synthesis of bioethanol and fibres [3-6]. Hemicellulose, polysaccharide consisting of much short-branched polymer chain of various type of saccharides, can be used to produce high value chemicals such as furfural, furan, and biopolymer[3, 4, 6]. Lignin is polyaromatic polymers consisting of vast aromatic structures connected with ether and carbon-carbon bonds and makes plant tissue soft and water resistance. Plant lignin can be used in the synthesis of aromatic compounds and polymers[4, 6, 7]. Thus, high volume of cellulose from SCB is a promising source for the preparation of micro- and nano-sized cellulose fiber aside from woods or cotton.

In early 20th century, micro- and nano-sized cellulose fibers were discovered and they were described as cellulose fibers which have at least one dimension in micro- and nanometer range[8-10]. Micro-sized cellulose fiber posted many excellent properties of cellulose polymer such as tensile strength, stiffness, thermal properties, and chemical and biological resistance[8, 9]. Nano-sized cellulose fiber properties are closer to perfect cellulose crystal than micro-sized cellulose, which are equivalent to a strong synthetic fibers, and much more environmentally friendly than petroleum-based polymer[8, 11, 12].

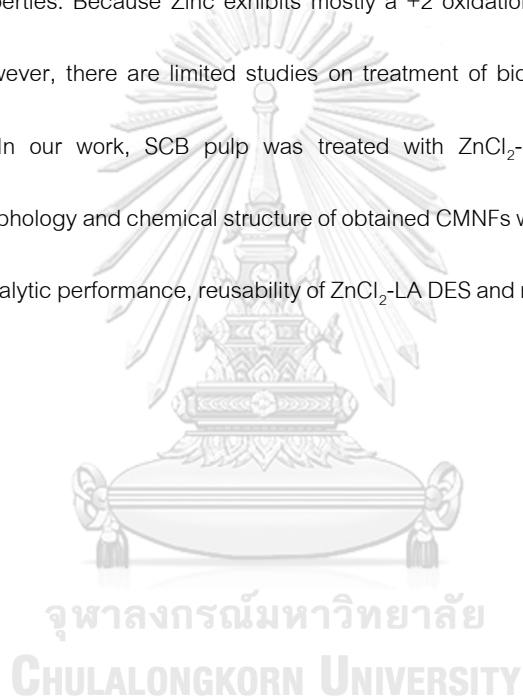
Preparation of cellulose micro- and nanofibers using green process is a challenging goal. Many of manufacturer use a chemical approach which involves a tremendous amount of strong acid and requires acid resistance equipment[13-15] or using a mechanical technique i.e., ball milling, high-speed homogenizer, microfluidization, and intensive ultrasonication. However, the obtained fiber still contains an amorphous region and gives the poor mechanical properties[8, 11, 12, 16]. Compared to other common procedures, cellulose micro- and nanofibers obtained from chemical pretreatment followed by low energy consumption mechanical disintegration were much more practical and environmentally friendly.

Pretreatment is a process that improves the cellulose fiber isolation by removing impurities, amorphous region, and breaking the cellulosic structure[16]. Chemical pretreatments are the most convenient and reliable processes. Alkali delignification and bleaching are general chemical pretreatments process used in pulp production. Chemical pretreatments require large quantity of chemical including acid, alkali, and organic solvent. Recently, greener solvents i.e., ionic liquids (ILs) and deep eutectic solvents (DESs) gain more attention in biomass pretreatment processes due to their low toxicity and recyclability. DES was discovered as a green solvent and has been gained a lot of attention in many research[14, 17-38]. DESs are mixtures of hydrogen bond donor (HBD) and hydrogen bond acceptor (HBA) and describe as a molten salt at room temperature which share lot of characteristics of ILs, but the preparation is much more practical and greener than ionic liquid[35]. DESs are useful in pretreatment of biopolymer, such as chitin or lignocellulose, their intermolecular bonding match with biological substances and make them available to disrupt the structure of biopolymer[14, 22, 32, 34]. Due to participation of Brønsted acid in DES, acidic reaction was found effective in cleavage of the cellulose chain to liberate the nanofibers[14, 20, 26, 34, 36]. Choline chloride (ChCl) and oxalic acid (OA) mixtures were acidic DES widely used in preparation of nano-sized cellulose from various sources and many techniques were combined to enhance the results[20, 21, 26, 29, 34, 36-38]. Another acidic DES, lactic acid (LA) - ChCl DES gave impressive results in delignification and preparation of cellulose nanofibers[14, 22, 25, 26, 32, 35]. There are number of works using urea or alcohol-based DES, but the use of



this type of DESs require intensive mechanical disintegration to liberate the cellulose nanofibers from sources[14, 22, 23, 32, 37]. Recently, acidic-catalyzed DESs were gained more attention, in order to perform experiment under milder conditions and improve the performance of DES[21, 24, 38].

Mixture of metal halides and HBDs are easy to prepare and give high catalytic performance DES[19, 31, 39]. This type of DES were deployed in many works to catalyze the reaction, for example, conversion of bioorganic compounds to high-value product[19].  $\text{ZnCl}_2$  is a metal halide with moderate-high catalytic activity due to Lewis acid properties. Because Zinc exhibits mostly a +2 oxidation state, it is easy to handled and recovered[31, 39]. However, there are limited studies on treatment of biomass with  $\text{ZnCl}_2$ -LA DES and its catalytic mechanism. In our work, SCB pulp was treated with  $\text{ZnCl}_2$ -LA DES followed by short time ultrasonication and morphology and chemical structure of obtained CMNFs were inspected by various method. Herein we report the catalytic performance, reusability of  $\text{ZnCl}_2$ -LA DES and recovery of zinc from the inefficient DES.



## CHAPTER II

### THEORY AND LITERATURE REVIEWS

#### 2.1. Sugarcane bagasse

Sugarcane bagasse (SCB) is a lignocellulosic agricultural byproduct from the sugar refining industry. Nearly 3 tons of the wet SCB is produced from every 10 tons of crushed sugarcane. Global consumption of table sugar generates SCB approximately 317-380 million tons per year. According to Thailand's SCB data, SCB generation from 2016 to 2018 are more than 30 million tons per year[40].

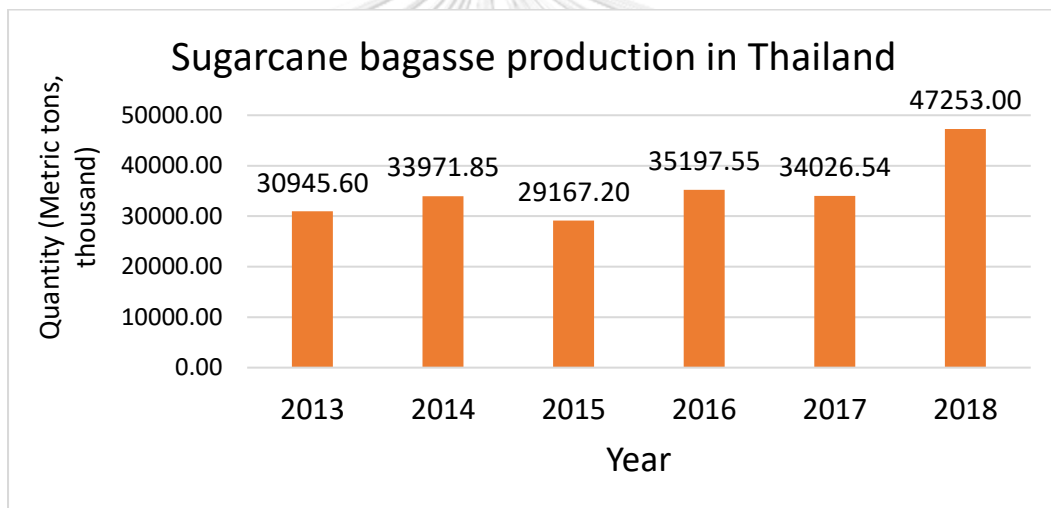


Figure 1. Thailand's production of sugarcane bagasse (thousand metric tons) [40].

#### 2.2. Lignocellulose

Lignocellulose is biomass which composed of cellulose (35-50%), hemicellulose (20-40%), and lignin (15-25%). Lignocellulose is the main component in plants and functions as supporting tissue of plants, it accounts for 30-50 % of dry weight of plants. Lignocellulose is widely distributed in crop residues i.e., bagasse, corn stover, wheat straw, wood chips, leaves, and dead branches.

### 2.2.1. Cellulose

Cellulose is biopolymer made from  $\beta$ -D-glucose; a monosaccharide formed through photosynthesis. The structure of cellulose is a linear homopolysaccharide joined together via  $\beta$ -1-4-glycosidic linkage. The repeating unit of cellulose is cellobiose, molecule consisting of two glucose residues. Cellulose molecules have 3 hydroxyl group for each glucose unit, made them have a strong tendency to form intra and intermolecular hydrogen bonds with neighbour chains.

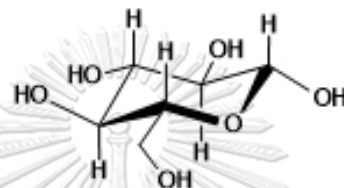


Figure 2. Chemical structure of  $\beta$ -D-glucose.

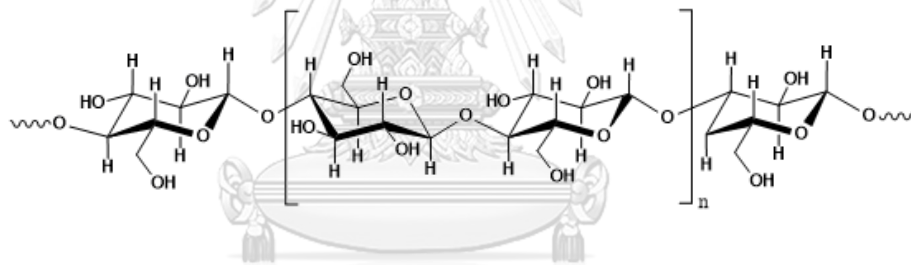


Figure 3. Chemical structure of cellulose polymer chain.

#### 2.2.1.1. Source

Most of cellulose was naturally produced by vascular plants but it can be found in various of organism i.e., algae, slime mold, and tunicates. Cellulose is produced from carbon fixation reaction in living organism 1.5 trillion tons every year.

### 2.2.1.2. Existence of Cellulose

Cellulose is located within the plant cell walls. Cellulose fibers obtained from different plants have different shapes and dimensions. Generally, the cell wall of the various plant fiber has a thickness of 4–6  $\mu\text{m}$  and divided into primary (P) and secondary (S) layers. The thin primary wall ( $\sim 100\text{ nm}$ ) of the plant fibers is developed first. The secondary wall has a thickness of 3–5  $\mu\text{m}$ , which is composed of three layers (S1, S2, and S3) and laid down inside the primary wall. The secondary layers are later developed, each sub-layers exhibiting different patterns due to orientation of microfibrils. The S2 layer occupies highest volume of cell wall and has typically 2–4  $\mu\text{m}$  thick. The S2 layer covers nanofibrillar bundles and lamellas, locating parallel to each other and located under an acute angle toward the fiber axis. This typical orientation has the greatest influence on properties of cell and macroscopic properties of the plant tissue. The S3 layer exhibits a helical winding pattern of microfibrils and lamellas. The lamellas of cell wall comprise of elementary nanofibrils having lateral size 3–15 nm and length of 1  $\mu\text{m}$ , that nanofibril contain well-ordered nanocrystallites.

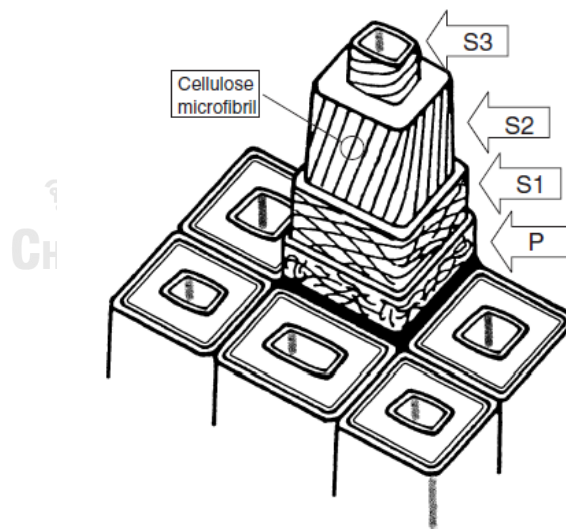


Figure 4. Plant cell wall structure [41].

### 2.2.1.3. Crystalline

Cellulose can be categorized into different types based on crystalline structure, which depends on cellulose chain packing arrangements. Major types of crystalline structure are cellulose I (monoclinic for  $I\beta$  and triclinic for  $I\alpha$ ) and cellulose II (monoclinic) [42]. All naturally occurred cellulose are cellulose I, cellulose II can be obtained from disordered cellulose I. Cellulose  $I\alpha$  is found mainly in bacterial cellulose and algae tissue, while cellulose  $I\beta$  is found in vascular plants and tunicates. The chain packing arrangements can be converted between one another, for example, cellulose  $I\alpha$  can be converted to cellulose  $I\beta$  by annealing to improve the stability of structure. The cellulose  $I\alpha$  has a one-chain triclinic unit cell, while cellulose  $I\beta$  has a two parallel chains monoclinic unit cell. The main different between two sub-allomorphs is how the hydrogen-bonded planes lie on top of each other.

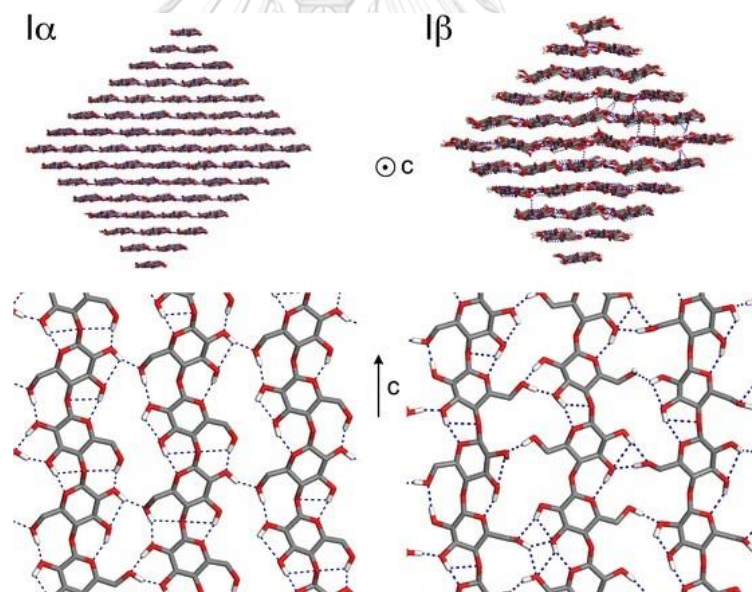


Figure 5. Cellulose crystalline lattice structure [42].

#### 2.2.1.4. H-bonding

In native cellulose molecules, there are three hydroxyl groups (OH) in the order of the polarity or reactivity, 2o-hydroxyl group at C-2, 1o-hydroxyl group at C-6 and 2o-hydroxyl group at C-3 position. Each hydroxyl group are equatorially bonded to glucopyranose ring. The OH--O hydrogen bonding dominates the cellulose intra-sheet interactions. The CH--O hydrogen bonding and van der Waals interaction are accountable for the weaker inter-sheet interaction.

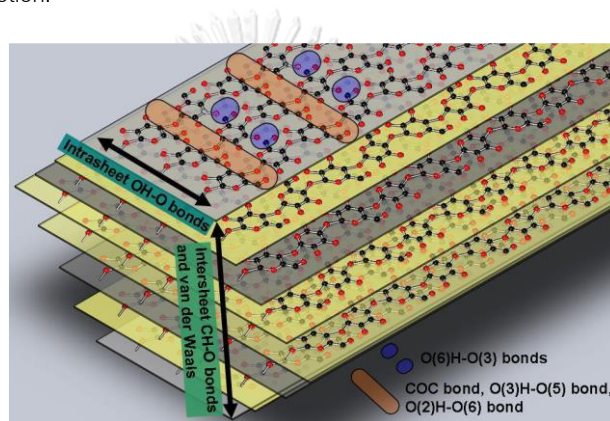


Figure 6. H-bonding between cellulose molecule [43].

The primary OH group at C-6 position has three possible conformations: *gt*, *tg*, and *gg* [43]. The most thermodynamically stable conformation is *gt* which represent 2/3 of total conformation. The *gg* is the only conformation that allows to forming inter-sheet hydrogen bond between OH group at C-6 position and oxygen atom at C-2 position.

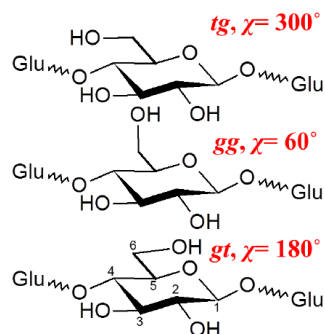


Figure 7. Conformation of C6-OH moiety in cellulose chain [43].

### 2.2.2. Hemicellulose

Hemicelluloses are second fundamental constituent of plant tissue and make up to 20-35 % of plant dry weight. Hemicelluloses are present in plant cell wall and offer structural strength by cross-linking between cellulose chain and lignin. Degree of polymerization of hemicellulose is lower, compare with that of cellulose. Hemicellulose chains contain sugar molecules with 500 to 3,000 units, whereas cellulose contains only glucose with 7,000 to 15,000 units per chain. Hemicellulose contains a diversity of glycosidic bonds in a single molecule, which makes them amorphous in nature and soluble in water. Hemicellulose can be divided into various categories, depending on the chemical structure and monomers i.e., xylan mannan, xyloglucan, and  $\beta$ -glucan linkages. Xylose is the main monomer followed by mannose, galactose, and glucose, whereas arabinose and rhamnose [44].

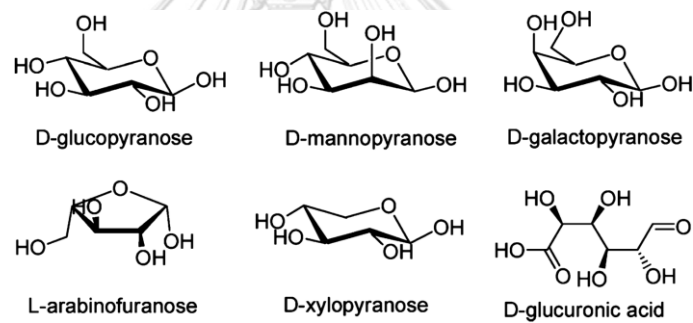


Figure 8. Hemicellulose's common monomers [44].

### 2.2.3. Lignin

Lignin is a biopolymer with a complex structure of polyphenols. About  $20 \times 10^9$  tons of lignin produced by vascular plants each year and typically found between the wood cells. Lignin is polyphenolic compounds composed with monolignols such as p-coumaryl alcohol and sinapyl alcohol bonded together through ether bond. Lignin monolignol is typically associated with the corresponding structural units such as the p-hydroxyphenyl unit, guaiacyl unit, and syringyl unit. The resulting lignin polymers possess unique properties, including resistance to chemical and biological decay, ultraviolet light absorption, and antioxidant activity

### 2.3. Nanocellulose

Nanocellulose are cellulose fiber with at least one dimension in nanometer range (less than 100 nm).

Nanocellulose possess unique characteristics, including biocompatibility, high specific surface area, biodegradability, high crystallinity, and low toxicity. According to length, width, aspect ratio, and composition, nanocellulose can be classified into five main categories as shown in Table 1.

**Table 1.** Classifications of nanocellulose and synthesis method[43].

Nanocellulose derivatives	Synthesis method	Morphological structure	Particle size
cellulose microfibrils	Mechanical treatment, enzymatic or chemical pretreatment	Long and thin fiber networks with crystalline and amorphous regions	Wide size range (micro to nano sizes)
cellulose nanofibers	Pressure-incremented homogenization, enzymatic and/or chemical treatment	Consists of both specific and accumulated nano-fibrils	Length: few Micrometers Fibril width: 10–100 nm
Bacterial cellulose nanofibers	Biosynthesis to produce bacterial-based nanocellulose	Ribbon-like nanofibers	Length: few micrometers Fibril width: 20–100 nm
Cellulose nanocrystals	Mechanical treatment without acid hydrolysis and sonication	Crystalline needle-like cellulose particles with 54–88% crystallinity	Length: 100–500 nm Fibril width: <100 nm
Spherical cellulose nanoparticles	Acidic treatment to precipitate and regenerate the dissolved amorphous cellulose	Spherical shape	Diameter: 50–100 nm



### 2.3.1. Cellulose microfibrils

Cellulose microfibrils (CMF) or microfibrillated celluloses (MFC) are micro-sized fibers that can be isolated from plant. CMF and MFC are generally fabricated from sources by using mechanical method, combination with biological or chemical pretreatment step can be used to improve accessibility of the fibrils. As a result, CMF and MFC contains amorphous region (hemicellulose and lignin) which can affect the properties and structure of the obtained fibers. CMF possess high yield stress, viscosity and water holding capacity. The main application of CMF and MFC are using as reinforce material in the textile and pulp industries.

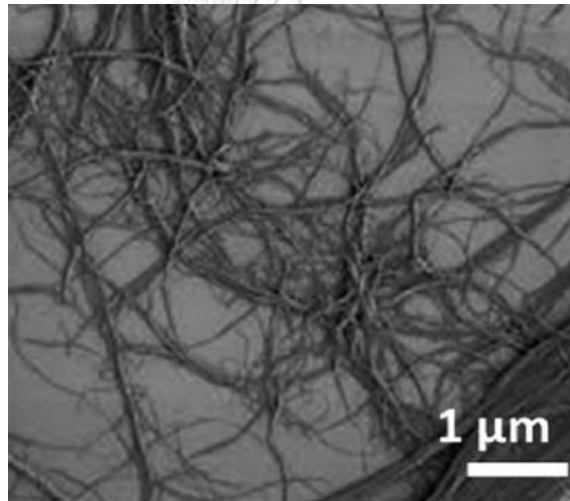


Figure 9. Scanning electron microscope (SEM) image of cellulose microfibrils[45].

### 2.3.2. Celluloses nanofibers

Cellulose nanofibers (CNFs) or Nanofibrillated celluloses (NFC) are cellulose fibrils with diameter ranges from 5 to 20 nm and the length from 0.5 to 2 μm. CNFs are web-like structure and contain both amorphous and crystalline parts. CNFs and NFC can be produced from various mechanical or chemical processes. Due to fibers high aspect ratio, CNFs are more flexible and larger surface area than any other fibers type. CNFs possess high strength (1-3 GPa) and high crystal modulus (138 GPa). The application of CNFs and NFC are using in food packaging, polymer reinforcement, tissue- engineering, and pharmaceutical application.

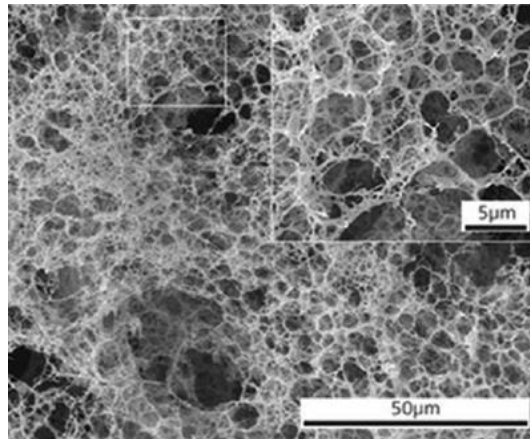


Figure 10. SEM image of cellulose nanofiber[45].

### 2.3.3. Bacterial cellulose nanofibers

Bacterial cellulose (BC) fibers are ribbon-shaped fibrils with  $\sim 100$  nm length and a diameter of 2 to 4 nm, forming a dense porous network[46]. Unlike plant derived nanofibers, BC fibers can be obtained in high yield and purity from certain types of bacteria (the most common are *Gluconacetobacter xylinus* and *Acetobacter xylinum*[46]) without require chemical processes for lignin and hemicellulose removal. The fibers possess high crystallinity (84-89%), high elastic modulus ( $\sim 78$  GPa), and extreme water holding capacity. BC fibers found useful in biomedical application, especially tissue and bone growth.

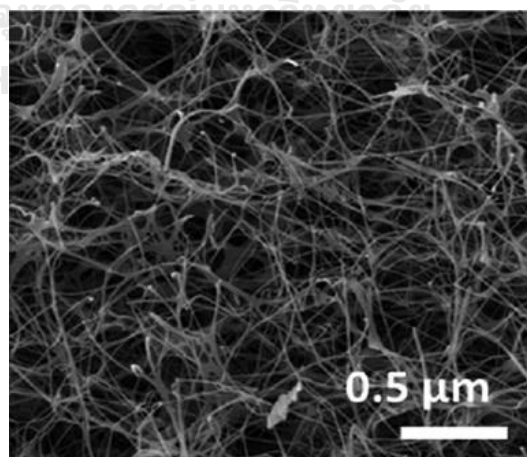


Figure 11. SEM image of bacterial cellulose nanofiber[45].

#### 2.3.4. Cellulose nanocrystals

Cellulose nanocrystals (CNCs), nanocrystalline celluloses (NCC), or cellulose nanowhiskers (CNWs) Are cellulose nanofibers with needle-like morphology. CNCs have diameter of 3-7 nm and 100 nm length[45]. CNCs are fabricated from various cellulosic materials. Preparation of CNCs involves acid hydrolysis of amorphous regions and improve the accessibility of fibers. Thus, resultant fibers represent a highly crystalline material. CNCs have a remarkable elastic modulus (up to 170 GPa) because of their high hydrogen bonding capacity[45], but CNCs are suffers from less flexibility due to their short and high crystallinity profile. CNCs are useful in reinforcement of polymeric nanocomposites and membrane applications.

#### 2.3.5. Spherical cellulose nanoparticles

Spherical cellulose nanoparticles (SCNPs) are spherical of amorphous or partial crystalline cellulose nanoparticles with diameter less than 100 nm[45]. SCNPs are produced by hydrolysis of microfibers with acid or enzyme, followed by regeneration of amorphous cellulose in water and disintegration into nanoparticles with ultrasonic disperser[45]. Due to their high amorphous structure, SCNPs display high sorption ability, high hydrophilicity, great amount of functional group, and high viscosity. These nanosphere can be used as toughening agents or catalyst supporting materials. SCNPs are used as filler in cosmetics, and medicine therapies, such as creams, sprays, and cream for skincare and cure.

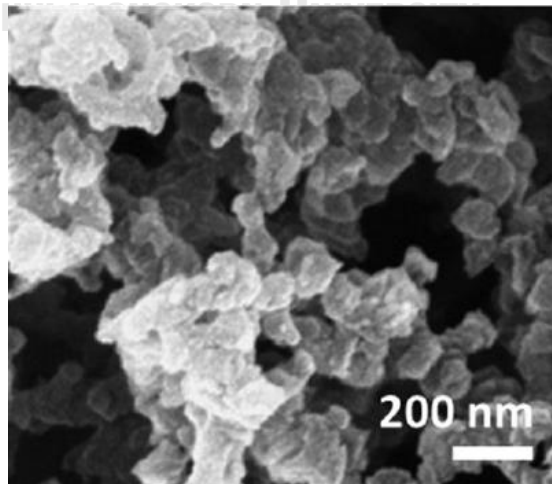


Figure 12. SEM image of spherical cellulose nanoparticles[45].

## 2.4. Nanocellulose fabrications

Preparation of cellulose nanomaterials mainly involves two steps (i) purification (ii) cellulose material separation. Sources of cellulose and processing protocols affect the structure, morphology, and properties of resultant nanomaterials. Generally, cellulose nanomaterials can be obtained by two main approaches Top-down and bottom-up approach.

### 2.4.1. Top-down approaches

Top-down approaches are those in which the bulk cellulose materials disintegrate into smaller size particles. The common top-down methods are mechanical disintegration, chemical treatment, and biological method.

#### 2.4.1.1. Mechanical disintegration

Mechanical disintegration is generally used to divide the cellulose pulp fibers into micro- of nanoscale particles. Mechanical disintegration is mainly concentrated within the fragile amorphous region of the cellulose fibrils while leaving the dense crystal regions strong and intact. The most common mechanical methods including high-pressure homogenization, cryo crushing, grinding, high intensity ultrasonication, microfluidization, and aqueous counter collision.

##### 2.4.1.1.1. High-pressure homogenization

High-pressure homogenization (HPH) is a method involves forcing the suspension through narrow channel (5-20  $\mu\text{m}$ ) with high pressure of 50 to 2,000 MPa. The gas bubble formation and implosion occur when the high-pressure suspension leaves the homogenization gap, induce the formation of shockwave and cavitations. The reduction of cellulose fiber can be obtained via large pressure drop, turbulent flow, high shear force, and particle collisions. The severity of fibers disruption depends on number of cycles and the applied pressure. HPH is convenience method which widely used method for large-scale production of CNF.

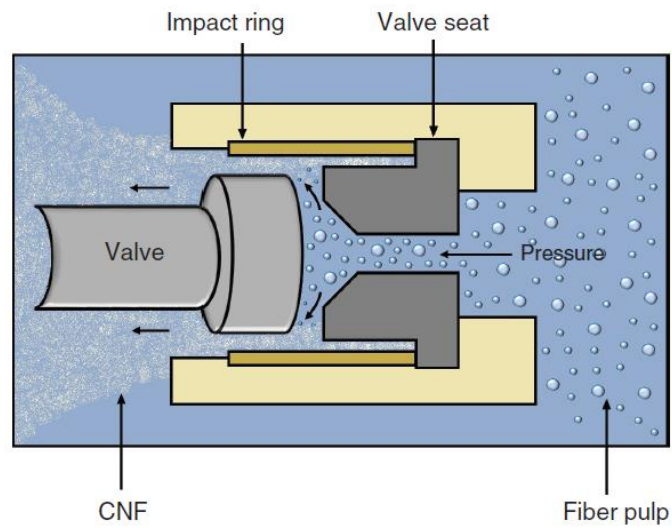


Figure 13. Equipment diagram and Mechanism of of high-pressure homogenization[45].

#### 2.4.1.1.2. Microfluidization

Microfluidizer is a tool that used for CNF and CMF preparation. The suspension is pumped through a Z-shaped chamber with high pressure as high as 276 MPa. The specially designed fixed-geometry microchannels are placed within the chamber, where the pulp slurry accelerates to high velocities and collides to the wall of the Z-shaped chamber. Cellulose fibers disrupt into smaller sized due to 3 types of forces: shear, impact, and energy dissipation.

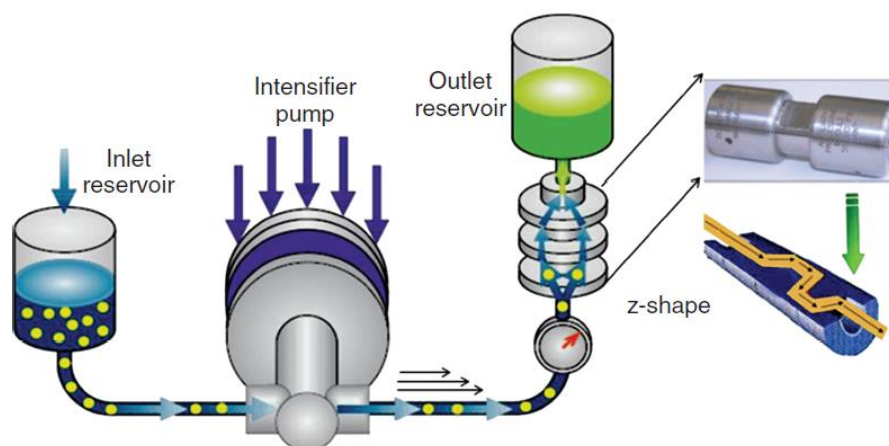


Figure 14. Equipment diagram of microfluidization technique[43].

#### 2.4.1.1.3. Grinding method

Grinding method is the fibrillation process uses shear forces to disintegrate the fibrils structure into nanoscale. Grinding is done by passing fiber slurry between static and rotating grindstones, which applies a shearing stress to fibers. The severity of fibrillation is dependent on the space between the disks, the morphology of the disk channels, and the number of passes through the grinder.

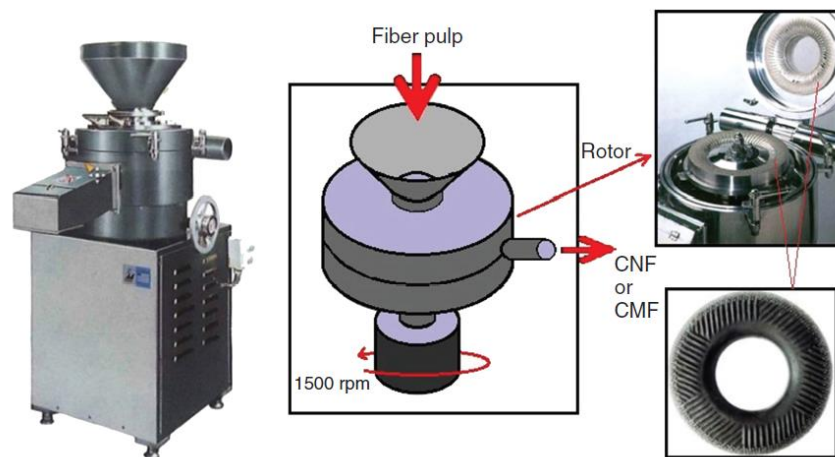


Figure 15. Equipment diagram show how grinding method works[43].

#### 2.4.1.1.4. Cryocrushing

Cryocrushing is mechanical fibrillation method in extremely low temperature. This method involves freezing of water-swollen cellulose in liquid nitrogen and subsequently crushed. The high impact forces to the icy cellulosic cellulose fibers leads to breakage of the plant cell walls and liberates the smaller fibers. This method fabricates fibrils with relatively large diameter (0.1-1  $\mu\text{m}$ ) [45].

#### 2.4.1.1.5. High-intensity ultrasonication

High-intensity ultrasonication (HIUS) is a common laboratory scale method for cell disruption using ultrasonic in aqueous medium. In principle, the high frequency is generated electronically and converted to mechanical energy in the sample via a metal probe that oscillate with high frequency (20-50 kHz). The high frequency oscillation initiates a localized high-pressure region resulting in formation, expansion, and implosion

of microscopic gas bubbles, leading to the defibrillation of the cellulose fibers. This method gives aggregated fibrils with a broad width distribution.

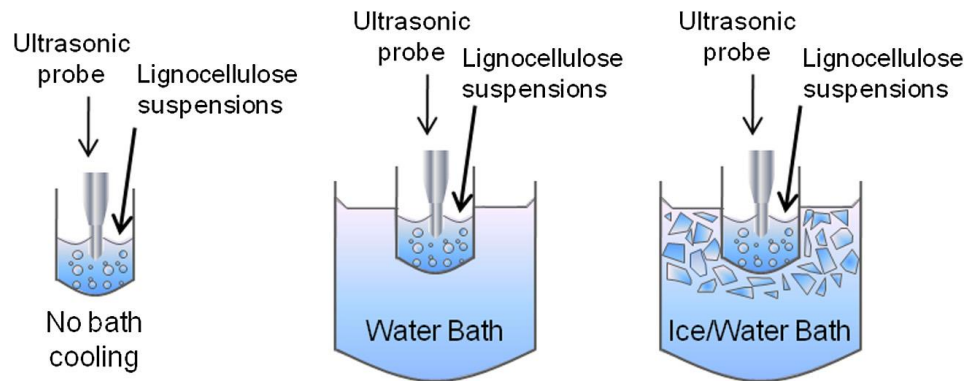


Figure 16. Defibrillation of lignocellulose fiber with high-intensity ultrasonication[45].

#### 2.4.1.1.6. Aqueous counter collision

Aqueous counter collision of ultrahigh-pressure water jet treatment, a method to prepare cellulose nanofibers by using jet counter collision apparatus subjecting cellulose suspension under ultrahigh-pressure (200 MPa). The fibrillation occurs due to shear force and particle collision. The resulting fibers has a width profile of several dozen nanometers and single to double digits micron of length.

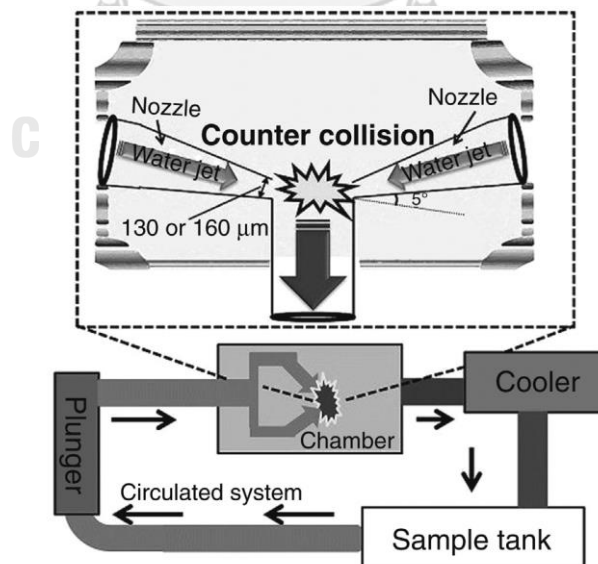


Figure 17. Equipment diagram of aqueous counter collision technique[45].

#### 2.4.1.1.7. Ball milling collision

Ball milling is a mechanical process used for preparation of CNFs. Principle of this method is using energy from collision between ball to break cellulose cell wall. The cellulose suspension is placed in a hollow cylindrical container. Inside the container is partially filled with balls made of ceramic, metal, or zirconia. The collision occurs due to container rotation and breaks cellulose fibers into smaller size.

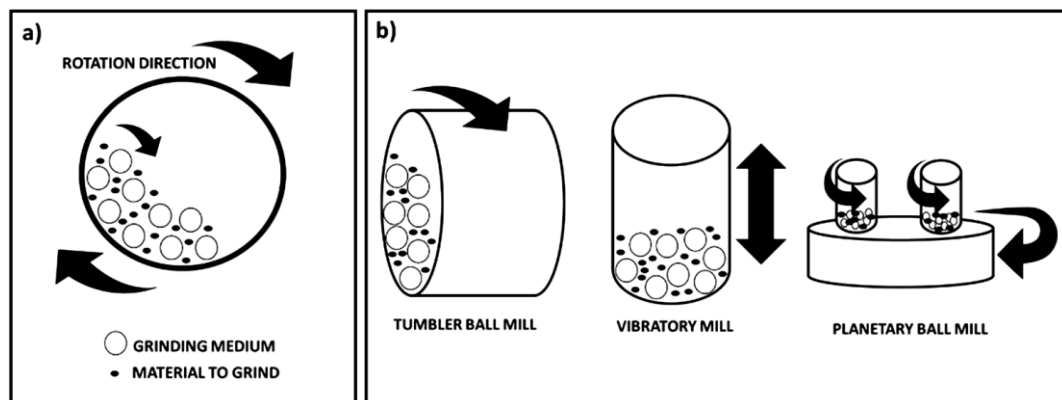


Figure 18. Diagrams show different type of grinding methods[45].

#### 2.4.1.2. Chemical treatment

Chemical treatment can be used as a single step or combined with mild mechanical fibrillation. Chemical treatment of native cellulose improves accessibility of the cellulose structure. Various chemical-based treatment methods including acid hydrolysis, surface modification, oxidation, and solvent pretreatment can be used for cellulose nanofibers preparation.

##### 2.4.1.2.1. Acid hydrolysis

Acid hydrolysis can be used to prepared CNC from the pulp fibers. This technique uses various mineral acids such as sulfuric acid ( $H_2SO_4$ ), hydrochloric acid (HCl), hydrobromic acid (HBr), and phosphoric acid ( $H_3PO_4$ ) to defibrillate cellulose fibers. Acid hydrolysis mainly remove the amorphous region and retains the crystalline parts of the fibers ending up with high crystallinity fibers production. Morphology and size of cellulose nanofibers depend on reaction duration, temperature, acid type and its concentration. Some acids



like  $\text{H}_2\text{SO}_4$  could form negatively charged nanocellulose fibers via sulfate group. The main disadvantage of acid hydrolysis includes corrosion, low recovery, and wastewater production.

#### 2.4.1.2.2. Hydrolysis with solid acid

Hydrolysis by solid acid is a technique design to overcome the problems of aqueous acid hydrolysis such as acidic corrosion of equipment, wastewater production, and consumption of energy and chemicals. Various type of solid acid such as acidic cation exchange resin and solid phosphor-tungsten acid ( $\text{H}_3\text{PW}_{12}\text{O}_{40}$ ) combine with high-power disintegration can be used to prepared cellulose nanomaterials[45]. The resultant nanomaterials exhibited a significantly higher thermal stability than CNCs prepared using aqueous acid hydrolysis. The major advantages of hydrolysis with solid acid are easy recovery of the solid acid, reusable, and low equipment corrosion. The drawbacks of this hydrolysis method are cost of solid acid, low productivity, and broad particle size distribution due to limited contact between solid acid and cellulose feed stock.

#### 2.4.1.2.3. Ionic liquid treatment

Ionic liquids (ILs) are molten salt at room temperature. ILs involve cellulose nanomaterials preparation via cellulose dissolution and hydrolysis of less order regions. Figure illustrates the dissolution mechanism of cellulose in ILs. Some examples of ILs which can dissolve cellulose are 1-butyl-3-methylimidazolium hydrogen sulfate ( $\text{BmimHSO}_4$ ), 1-butyl- 3-methylimidazolium chloride ( $\text{BmimCl}$ ), 1-allyl-3-methylimidazolium chloride ( $\text{AmimCl}$ ), and 1-butyl-3-methylimidazolium acetate ( $\text{BmimOAc}$ ) [45].

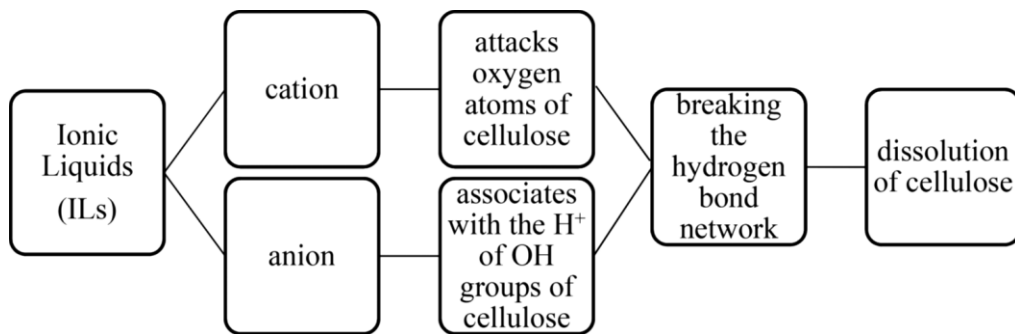


Figure 19. diagram show dissolution mechanism of cellulose in ILs.

#### 2.4.1.2.4. TEMPO oxidation

TEMPO oxidation method, the process involved the functionalization of carboxylate and aldehyde onto the cellulose structure by using oxidizing agent. The oxidizing reagent used in this method are sodium hypochlorite ( $\text{NaOCl}$ ) in the presence of 2,2,6,6-tetramethyl-1-piperidine-N-oxyl (TEMPO) radical and iodine or bromine as catalyst. The oxidation occurs only at the surface of fibers. Resultants oxidized product has negative charge surface and resulted in repulsion between fibrils, thus fibrillation of cellulose occurred easily.

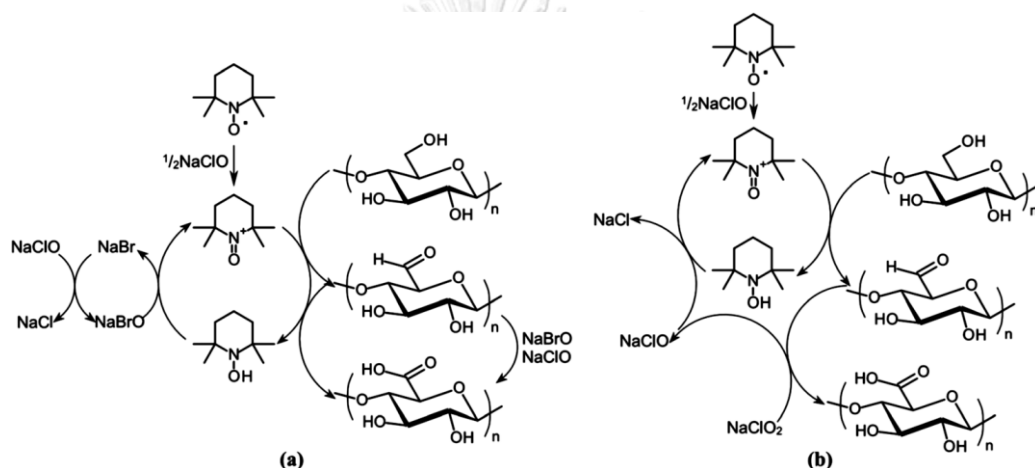


Figure 20. diagram show mechanism of cellulose oxidation with TEMPO[45].

#### 2.4.1.3. Enzymatic pretreatment

Enzymatic pretreatment is a top-down biological treatment that used enzymatic degradation of non-cellulosic contents and low-ordered cellulosic structure. In this method, enzymes are used in the assistance of the elimination of non-cellulosic substances or selectively hydrolysis of amorphous cellulose region. As a single enzyme can't degrade all the cellulosic fibers, three common enzymes used for this pretreatment process are:

(1) endoglucanases or  $\beta$ -1,4-endoglucanases[46]: The cellulase which randomly hydrolyze intramolecular  $\beta$ -1,4-glucosidic bonds in cellulose chains and generates various lengths of cellulose fibers.

(2) exoglucanases (cellobiohydrolases)[46]: The cellulase which hydrolyze on the crystalline chain termini and release cellobiose and glucose as major products.

(3)  $\beta$ -glucosidases[46]: The enzyme which eliminate cellobiose inhibition by hydrolyze cellobiose into glucose.

#### 2.4.2. Bottom-up approaches

Bottom-up approaches are those where the nanostructures of the fibers fabricated from molecular scale sources, such as regeneration of cellulose nanofibers from dissolve cellulose.

##### 2.4.2.1. Electrospinning

Electrospinning is method for producing micro- and nanofibers from polymer solution. The solution of cellulose is prepared by specific solvent. Under the high electrostatic voltage, the polymer solution deforms due to the repulsion of identical charges at the surface of the drop. The surface of the solution is distorted into conical shape. Once the voltage exceeds the surface tension of the polymer, a liquid jet is then ejected from the cone tip. As the fine jet travels through the air, the solvent is evaporated and leaving ultrafine polymeric fibers on the grounded collector. Resultant fibers have diameters of 100 to 1000 nm. Figure..... shown a schematic of the electro spinning process.

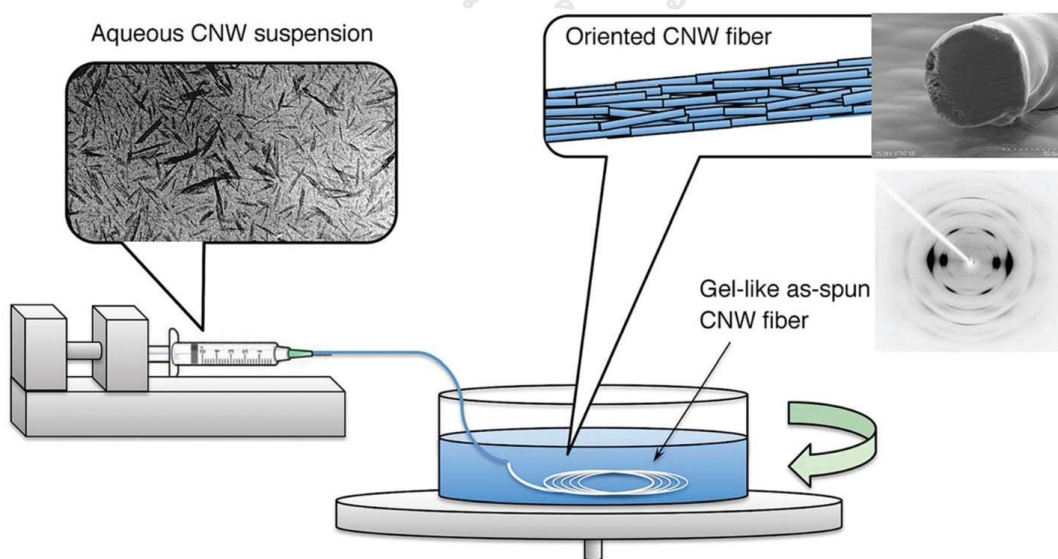


Figure 21. Preparation of cellulose nanofibers with electrospinning method[45].

#### 2.4.2.2. Bacterial biosynthesis

Bacterial biosynthesis is a method for producing bacterial cellulose by certain bacteria. Bacteria consume low-molecular-weight sugars and excrete cellulose nanofibers into the aqueous culture medium. The resultant cellulose fibers have a ribbon shape and form a 3D nanofiber network. Simple purification processes are required to obtain extremely pure cellulose fibers [45].

#### 2.5. Deep eutectic solvents

Deep eutectic solvents are eutectic mixtures with their eutectic points lower than that of the ideal liquid mixture. DESs are mixtures of hydrogen bond donor (HBD) and hydrogen bond acceptor (HBA) at different ratios to give a room temperature liquid mixture. Figure 22 shows several common salts as HBAs and HBDs used to make DESs. DESs contain ionic components such as metal salts and are considered as ionic liquid (IL) analogues, since they have some similarities with ILs. DESs are classified in Table 2 based on the nature of their HBDs and HBAs. Type I DESs are made up of quaternary ammonium salts and anhydrous metal halides with a general formula of  $\text{Cat}^+ \text{X}^- \text{zMCl}_x$  where  $\text{X}^-$  is a Lewis base ( $x$  and  $z$  refer to the number of  $\text{Cl}^-$  and  $\text{MCl}_x$ , respectively). Type II DESs contain a mixture of hydrate metal halides and quaternary ammonium salts with a common formula of  $\text{Cat}^+ \text{X}^- \text{zMCl}_x \cdot y\text{H}_2\text{O}$  ( $y$  refers to the number of water molecules). Type III DESs are made of quaternary ammonium salts and HBDs such as alcohols, amides, and carboxylic acids. Type IV DESs are made of HBDs mixed with metal halides.

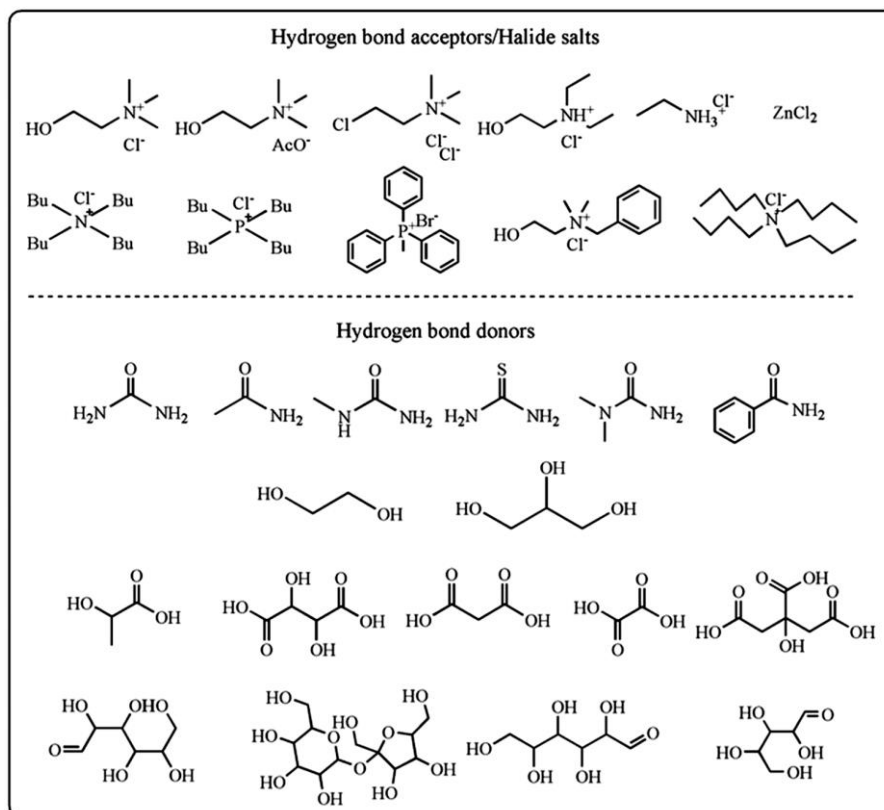


Figure 22. Shows different chemicals using as hydrogen bond acceptor and hydrogen bond donor[47].

Table 2. Type of DESs[47].

Type	Combination	General formula
Type I	Quaternary ammonium salt + metal chloride	$Cat^+X^- zMCl_x$
Type II	Quaternary ammonium salt + metal chloride hydrate	$Cat^+X^- zMCl_x \cdot yH_2O$
Type III	Quaternary ammonium salt + hydrogen bond donor	$Cat^+X^- zRZ$
Type IV	Metal chloride hydrate + hydrogen bond donor	$MCl_x + RZ = MCl_{(x-1)}^+ \cdot RZ + MCl_{x+1}^-$

## 2.6. Literatures survey

In 2018, Sirviö, J. A. et al. [33] studied the fabrication of cellulose nanoparticles from regenerated cellulose from deep eutectic solvent. The DES based on guanidine hydrochloride and anhydrous phosphoric acid (molar ration 1:2) was used to dissolve cellulose at room temperature. Cellulose fibers were regenerated in water and fabricated into nanoparticles with microfluidizer. The obtained fibers have diameter of 6 nm and the crystallinity

changed from cellulose I to cellulose II. Regenerated cellulose nanoparticles were used as fillers and improved the elongation, tensile strength, and modulus of poly(vinylalcohol) composite films.

In 2019, Ma Y. et al. [29] prepared nanocellulose by pretreated kraft pulp with hydrated DES followed by ultrasonication. The pretreatment processes were used Choline chloride and oxalic acid dihydrate (molar ration 1:1) DES mixed with water at volume concentrations of 10, 20, and 30%. The pretreatment temperature was 80 °C and 1 h of reaction time. The obtained fibers were then fibrillated with ultrasonic treatment and resulted in CNF and CNC from processes.

In 2019, Yang X. et al. [38] studied the preparation of CNCs with thermally stable properties. CNCs were prepared from bleached eucalyptus kraft pulp (BEKP) treated with FeCl<sub>3</sub>-catalyzed deep eutectic solvent (F-DES). The F-DES was composed of oxalic acid dihydrate, choline chloride, and iron (III) chloride hexahydrate (FeCl<sub>3</sub>·6H<sub>2</sub>O) in a mass ratio of 4:1:0.2. BEKP was treated with one-step F-DES at mild condition (80 °C, 6 h) and resulted in high yield of CNCs (over 90% based on cellulose content). The resultant CNCs with a diameter range of 5-20 nm and 50-300 nm length were showed high thermal stability (onset thermal degradation higher than 310 °C).

In 2020, Li X. et. al [24] studied the improvement of dissolution of cotton cellulose in 1-allyl-3-methylimidazolium chloride (AmimCl) by addition of metal chlorides. The cotton cellulose fibers were dissolve with AmimCl ionic liquid. Addition of metal chlorides were introduced the interaction between metal cations with hydroxyl oxygen and destroyed intermolecular hydrogen bonds of cellulose structure. The addition of ZnCl<sub>2</sub> was reduced the dissolution time from 52 to 5 minutes and increased the maximum solubility of cotton cellulose in AmimCl by 1.37 times at 80 °C.

In 2020, Wang H. et al. [36] prepared CNCs from cotton fibers by using DES pretreatment followed by high-pressure homogenization. The DES based on choline chloride and oxalic acid dihydrate (molar ration of 1:1) was used for pretreatment of cotton fibers at 100 °C for 6 h. The obtained fibers were then subjected to high-pressure homogenizer at 100 MPa for 30 min. Resultants CNCs with diameter range of 50-100 nm and

500-800 nm length and high crystallinity (77.6%) were obtained. The DES can be recycled for 3 pretreatment cycles.

In 2020, Jiang J. et al. [21] prepared lignin-containing cellulose nanocrystals (LCNCs) by using ternary deep eutectic solvents followed by mild mechanical blending. The ternary DES are based on choline chloride, oxalic acid, and *p*-toluenesulfonic acid (2:1:1 molar ratio). They obtained high yield (66%) of LCNCs with 6 nm width and 3.3 nm thickness after pretreatment at 80 °C for 3 h followed by 30 min of mechanical blending. The LCNCs were contained high amount of lignin (47.8%) and retained cellulose I crystallinity (57.4%).

In 2020, Li P. et al. [23] studied the preparation of cellulose nanofibrils from urea-based DES. In this work, DESs based on urea/guanidine hydrochloride (1:2 molar ration) and urea/ammonium thiocyanate (1:2 molar ratio) were prepared and used for pretreatment of bleached birch kraft paper. The pretreatment was done at 100 °C for 2 h and the obtained fibers were fabricated with high-speed homogenizer. The resultant fibers were cellulose nanofibrils with 13-19.3 nm width. The translucent nanofibril films made from pretreated cellulose fiber had a good thermal stability with tensile strengths of 135-189 MPa and elastic modulus of 6.4-7.7 GPa.

In 2020, Serrano M. L. et al. [48] studied the improvement of hydrolysis rate of cellulose after pretreatment of inorganic salt hydrates. Inorganic salt hydrates such as  $\text{ZnCl}_2 \cdot 4\text{H}_2\text{O}$ ,  $\text{ZnBr}_2 \cdot 4\text{H}_2\text{O}$ ,  $\text{LiCl} \cdot 8\text{H}_2\text{O}$  and  $\text{LiBr} \cdot 4\text{H}_2\text{O}$  were studied as a solvent for dissolution/precipitation pretreatment of cellulose. The dissolution of cellulose was very fast at 70 °C, cellulose dissolved in 15 minutes. The dissolution/precipitation was dramatically deconstructed the cellulose structure. They found that bromide salt hydrates are more efficient and dissolve cellulose faster than chloride salts. The obtained cellulose fibers after precipitation were then hydrolyzed by solid acid  $\text{H}_4\text{SiW}_{12}\text{O}_{40}$  (0.05 M) at 140 °C for 300 min and yield up to 90% of glucose.

In 2021, Liu S. et al. [26] studied the preparation of esterified cellulose nanofibers via acid based deep eutectic solvent treatment. The CNF was prepared from hardwood bleached kraft pulp by treated with

various DESs at 50 to 100 °C for 3 hours followed by mechanical extrusion for 3 times and colloid mill dispersion for 40 minutes. The results showed the optimum temperature for DESs pretreatment is higher than 85 °C. The obtained esterified CNFs exhibited yield of 72-88% and degree of polymerizations of 300-500 and maintain the cellulose I structure.

In 2021, Chen Y. et al. [14] studied dissolution mechanism of cellulose in various chloride salts. The successful and efficient cellulose dissolution of cellulose in  $\text{ZnCl}_2 \cdot 3\text{H}_2\text{O}$  and  $\text{FeCl}_3 \cdot 6\text{H}_2\text{O}$  were achieved in short time.  $\text{Zn}^{2+}$  and  $\text{Fe}^{3+}$  ions were broken intermolecular hydrogen bond. The abundant  $\text{H}^+$  in the metal chloride salts solution were attacked the  $\beta$ -1-4-glycosidic bonds to disintegration of cellulose chain.





## CHAPTER III EXPERIMENTAL

### 3.1. Materials

#### 3.1.1. Sugarcane Bagasse

Air dried sugarcane bagasse was obtained from Mitr Phol Co., Ltd.

#### 3.1.2. Chemicals

- 1) L-(+)-Lactic acid, Pharmaceutical (Carlo Erba)
- 2) zinc chloride,  $ZnCl_2$ , anhydrous (Carlo Erba)
- 3) oxalic acid (commercial grade)
- 4) Acetone (commercial grade)
- 5) Hydrogen peroxide 50% (commercial grade)
- 6) sodium hydroxide, NaOH (commercial grade)
- 7) Methanol-d4 (NMR spectroscopy grade (Merck))

### 3.2. Glassware and equipment

- 1) Oil bath
- 2) Hot plate with magnetic stirrer
- 3) rotary evaporator
- 4) Thermometer
- 5) Beaker
- 6) Laboratory bottle
- 7) Filter paper
- 8) Vacuum and pressure chamber
- 9) Vacuum pump

### 3.3. Instruments

- 1) Polarized Light Microscope
- 2) Fourier Transform Infrared Spectrophotometer
- 3) X-Ray Diffractometer
- 4) Transmission Electron Microscope
- 5) Nuclear magnetic resonance
- 6) Transmission electron microscope
- 7) Zetasizer

### 3.4. Experimental Procedures

#### 3.4.1. Preparation of sugarcane bagasse pulp

SCB pulp was prepared by general alkali delignification followed by peroxide bleaching procedure [2]. In brief, air dried sugarcane bagasse (50 g) was boiled in DI water (1000 mL) to remove water soluble impurities and ashes follow by delignified by sodium hydroxide (4 wt.%, 1000 mL) at 100 °C for 3 h. The delignified SCB was then suspended in fresh sodium hydroxide (4 wt.%, 500 mL) with continuous agitated at 500 rpm and a 15% H<sub>2</sub>O<sub>2</sub> solution (500 mL) was slowly added. After no bubbling in the bleaching suspension, the bleached SCB was filtered out and washed with deionized water. The bleaching process was repeated until white pulp was obtained.

#### 3.4.2. Preparation of ZnCl<sub>2</sub>-LA DES

ZnCl<sub>2</sub>:LA DES was prepared by mixing a 1:8 molar ratio of zinc chloride and lactic acid and heated at 60 °C with continuous stirring until a transparent solvent was formed.

#### 3.4.3. Fabrication of CMNFs

The SCB pulp (1 g) was added into and ZnCl<sub>2</sub>-LA DES (15 g) in 50 mL round bottom flask and heated in oil bath at 110 °C for 2 h with continuously stirring. The treated fibers were filtered through filter paper and washed with acetone/DI water (50%, 100mL) followed by DI water (100 mL). The treated SCB pulp was suspended in

deionized water to form total 60 mL of suspension and subjected to ultrasonic fiber disintegration using a titanium alloy probe tip (13 mm of diameter) (Qsonica, Q700, USA), frequency 20 kHz, amplitude 50%, and 30/10 s on/off pulse for 10 minutes. During ultrasonication, temperature of the suspension was suppressed by cooling with room temperature water. After resulting in a gel-like mixture, it was kept in bottle and stored in fridge for further study.

#### 3.4.4. Preparation of neat lactic acid pretreated fibers

1 g of SCB pulp and 25 g of lactic acid in round bottom flask were heated in oil bath at 120 °C for 2 h with continuously stirring. Mixture was filtered and washed with DI water (150 mL). Then, the treated SCB pulp was suspended in deionized water to formed total 60 mL of suspension and treated with ultrasonic with the same setting as CMNF.

#### 3.4.5. Reusing of ZnCl<sub>2</sub>-LA DES

The filtrate from the fabrication of CMNFs were evaporated *in vacuo* to remove to give the yellow-orange solution. DI water and fine powdered of activated carbon was then added into the solution. After agitation for 24 h, the activated carbon along with undissolved organic matters was filtered out and water in the filtrate was removed *in vacuo* to give the reusable ZnCl<sub>2</sub>-LA DES.

#### 3.4.6. Recover of Zinc

Acetone in the filtrate of used ZnCl<sub>2</sub>-LA DES (100 mL) was removed by evaporation *in vacuo* and some activated carbon was added to decolorize the DES. Then, the filtrate was collected, and oxalic acid (1M, 50mL) was added in the used DES. After zinc oxalate complexes were precipitated from solution, the precipitated zinc oxalate was filtered out and dried. The filtrate contains saccharides and lactic acid which is safe to disposed after neutralization of acid residues.

### 3.5. Characterizations

#### 3.5.1. Polarized light Microscopy

Fibers were suspended in DI water and a drop of suspension was placed on microscope slide and covered with cover slip. The appearance of pretreated fibers and CMNFs were observed under optical microscope (OLYMPUS BX53). The magnification used was 40x.

#### 3.5.2. Fourier transform infrared spectroscopy

The chemical functional groups and structures of cellulose fibers were inspected with FTIR spectrometer (Nicolet 6700), and the spectra were recorded in range 650 to 4000  $\text{cm}^{-1}$  with resolution of 4  $\text{cm}^{-1}$  and 64 scans.

#### 3.5.3. X-Ray diffraction

The crystal polymorphism of CMNFs were analyzed by X-ray powder diffraction analysis (Bruker D8 Discover) with Cu  $K\alpha$  radiation. The scanning angle ranged from  $2\theta = 5^\circ$  to  $40^\circ$ . The crystallinity index (CrI, %) of the obtained CMNF were calculated by using Segal method[49].

$$\text{CrI (\%)} = \left( \frac{I_{200} - I_{\text{am}}}{I_{200}} \right) \times 100\%$$

where, CrI is crystallinity index,  $I_{200}$  is peak intensity of plane (200), and  $I_{\text{am}}$  is the intensity at the valley between plane (200) and (110).

#### 3.5.4. Transmission electron microscopy

The dilute suspension of CMNF was deposited on TEM grid and stained with 1% uranyl acetate solution to increase the contrast of the images. The stained samples were observed under JEOL JEM-1400 Transmission Electron Microscope.

#### 3.5.5. $^{13}\text{C}$ and $^1\text{H}$ nuclear magnetic resonance spectroscopy

The sample of Lactic acid,  $\text{ZnCl}_2$ -LA DES, and reused  $\text{ZnCl}_2$ -LA DES were prepared by dissolving 50 mg of sample in deuterated methanol (methanol- $d_4$ ). The  $^1\text{H}$  and  $^{13}\text{C}$  spectra were recorded on 500 MHz Jeol JNM-

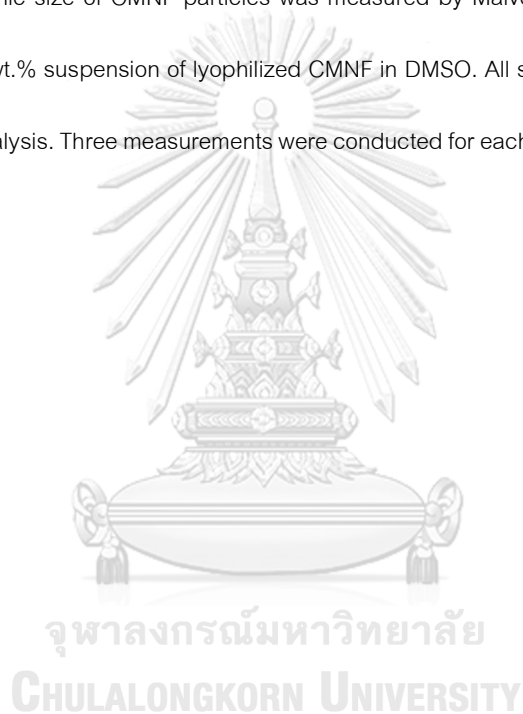
ECZ 500R NMR spectrometer. Solvent residual peak was referenced at 3.31 ppm for  $^1\text{H}$  and 49.00 ppm for  $^{13}\text{C}$ .

### 3.5.6. $^{13}\text{C}$ CP/MAS solid NMR spectroscopy

Freeze dried CMNF samples were grounded into fine powder and packed into rotor. NMR spectra were recorded on a 400 MHz Bruker Ascend NMR.

### 3.5.7. Dynamic light scattering

Average hydrodynamic size of CMNF particles was measured by Malvern Zetasizer nano ZSP. Samples were prepared as 0.1 wt.% suspension of lyophilized CMNF in DMSO. All sample were ultrasonically treated for 5 minutes before analysis. Three measurements were conducted for each sample and the mean of average size was reported.



## CHAPTER IV

### RESULTS AND DISCUSSION

#### 4.1 Preparation of sugarcane bagasse pulp

Sugarcane bagasse was prepared as pulp fibre through conventional processes, including alkali delignification and peroxide bleaching steps. Fibre's physical and chemical properties were then investigated with FTIR, optical microscope, and SEM.

In Figure 23, we have shown the dried bagasse chips we received from our supplier. The raw bagasse was washed with hot DI water to remove inorganic substances and insoluble solids, such as sand and dust. The raw bagasse was then dried in an oven overnight and characterized with FTIR.



Figure 23. Raw sugarcane bagasse.

The FTIR spectra showed that the initial raw bagasse contains cellulose, hemicellulose and lignin as we expected. In Figure 24(a), was shown the characteristic absorption spectrum of dried raw bagasse. The band at  $835.13\text{ cm}^{-1}$  is characteristic absorption of syringyl lignin and absorption at  $895.55\text{ cm}^{-1}$  is characteristic absorption of the C-O-C glycosidic bond in the cellulose chain. The region between  $1000$  to  $1200\text{ cm}^{-1}$  is a large contribution of C-O stretching from cellulose and hemicellulose, which exhibits a maximum value at  $1031.74\text{ cm}^{-1}$  due to C-O stretching and at  $1160.35\text{ cm}^{-1}$  for the asymmetrical stretching of C-O-C. The absorptions at  $1242.35$ ,  $1511.65$ ,  $1603.15$ , and  $1732.62\text{ cm}^{-1}$  are absorption of C-O stretching of hemicellulose and lignin, C=C stretching of aromatic rings, C=C and C=O stretching of aromatic rings and C=O stretching from hemicellulose moieties respectively. Furthermore, absorptions around  $2850$  to  $2916\text{ cm}^{-1}$  are absorption of  $\text{CH}_2$  stretching and absorption around  $3337.47\text{ cm}^{-1}$  is from -OH stretching of the hydroxyl group. In Figure 24(b), FTIR spectra of washed bagasse, there are absorption of cellulose characteristics peaks at wavenumber  $895.26$ ,  $1033.01$ ,  $1160.98$ ,  $1371.35$ , and  $1424.37\text{ cm}^{-1}$ . The spectra have shown the decreased peak at wavenumbers of  $835.13$ ,  $1242.63$ ,  $1511.65$ ,  $1603.15$ , and  $1743.62\text{ cm}^{-1}$  which are the absorptions of hemicellulose and lignin. As mentioned before, the hemicellulose is a polysaccharide consisting of various monosaccharides, which are mainly carboxylated molecules that can be hydrolyzed into water-soluble compounds. The bagasse was then delignified with hot sodium hydroxide and purified by bleaching with hydrogen peroxide in sodium hydroxide solution to achieve high-purity cellulose fiber. The FTIR spectra of bagasse pulp have shown the absence of lignin and hemicellulose characteristic absorptions. In Figure 25, the final bleached bagasse pulp appearance is white fluffy fibers with a cotton-like texture but obviously finer molecular size. Furthermore, we have conducted additional microscope analysis to observe structure and particle size under polarized microscope as shown in Figure 26.

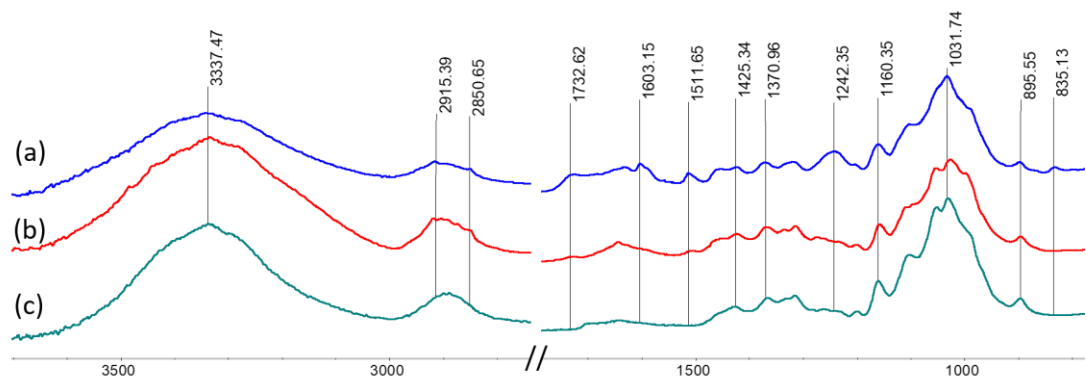


Figure 24. FTIR spectra of (a) raw bagasse, (b) DI water washed bagasse, (c) bleached bagasse pulp.



Figure 25. Appearance of bleached bagasse pulp.

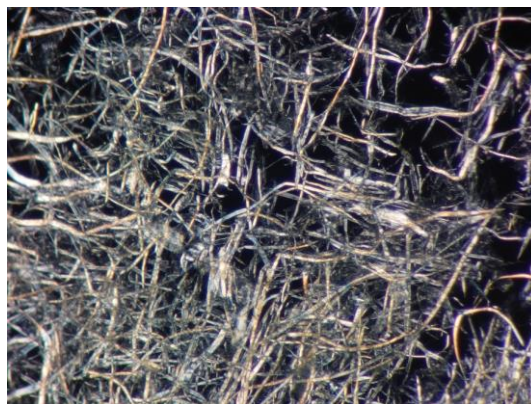


Figure 26. Bleached bagasse pulp under polarized-light microscope.



#### 4.2 Preparation of ZnCl<sub>2</sub>-LA DES

ZnCl<sub>2</sub>-LA DES was prepared by directly dissolving ZnCl<sub>2</sub> in a lactic acid solution. The exothermic reaction was occurred due to the breaking and bonding of intermolecular interaction without any change in chemical structures. Low heating was introduced into the reaction to lower mixture viscosity and accelerate the mixing step resulting in a clear viscous liquid with a slightly yellow to colourless appearance (Figure 27).

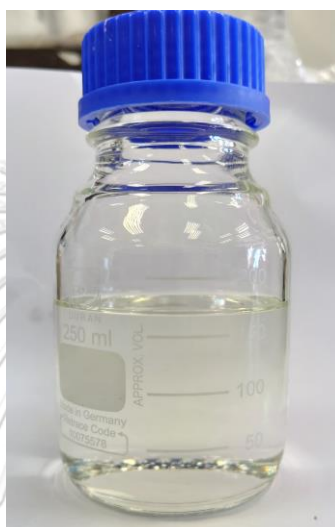


Figure 27. Appearance of ZnCl<sub>2</sub>-LA DES.

##### 4.2.1. NMR analysis

On basis of <sup>1</sup>H NMR spectra (Figure 28), the neat lactic acid showed a doublet signal ( $J = 7$  Hz) of CH<sub>3</sub> at  $\delta_{\text{H}}$  1.38 ppm and a quartet signal ( $J = 7$  Hz) of CH at  $\delta_{\text{H}}$  4.23 ppm and a presence of small amount peaks from lactic acid oligomers (Figure 28a.). For ZnCl<sub>2</sub>-LA DES (Figure 28b.), the chemical shifts of CH<sub>3</sub> and CH protons were slightly downfield-shifted which could indicate that the electron density of protons was shifted-away from nucleus due to the positive charge of Zn<sup>2+</sup> ions bound to the molecule.

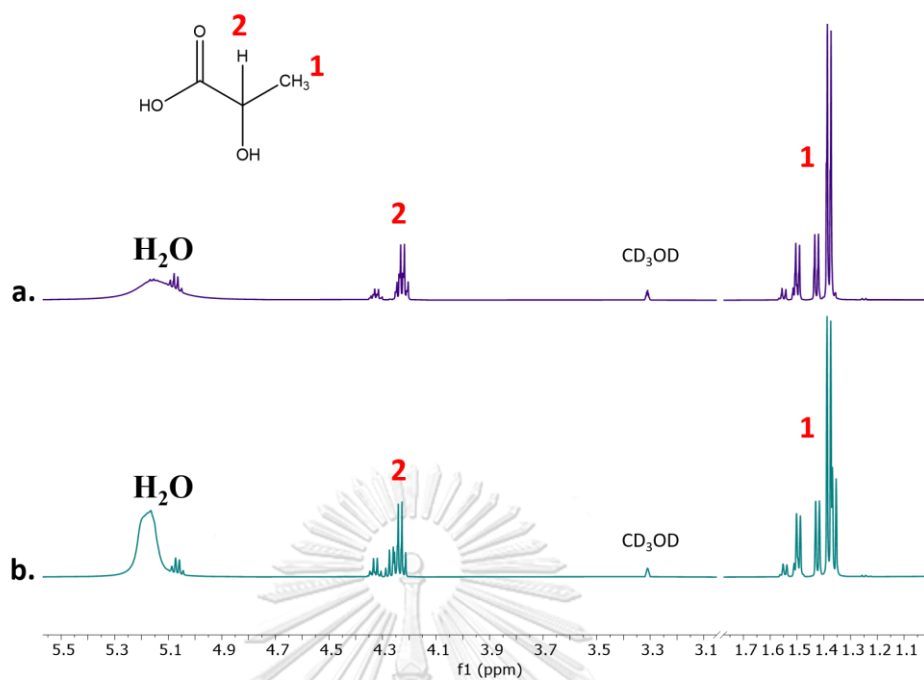


Figure 28.  $^1\text{H}$  NMR spectra of a. lactic acid and b. ZnCl<sub>2</sub>-LA DES in CD<sub>3</sub>OD.

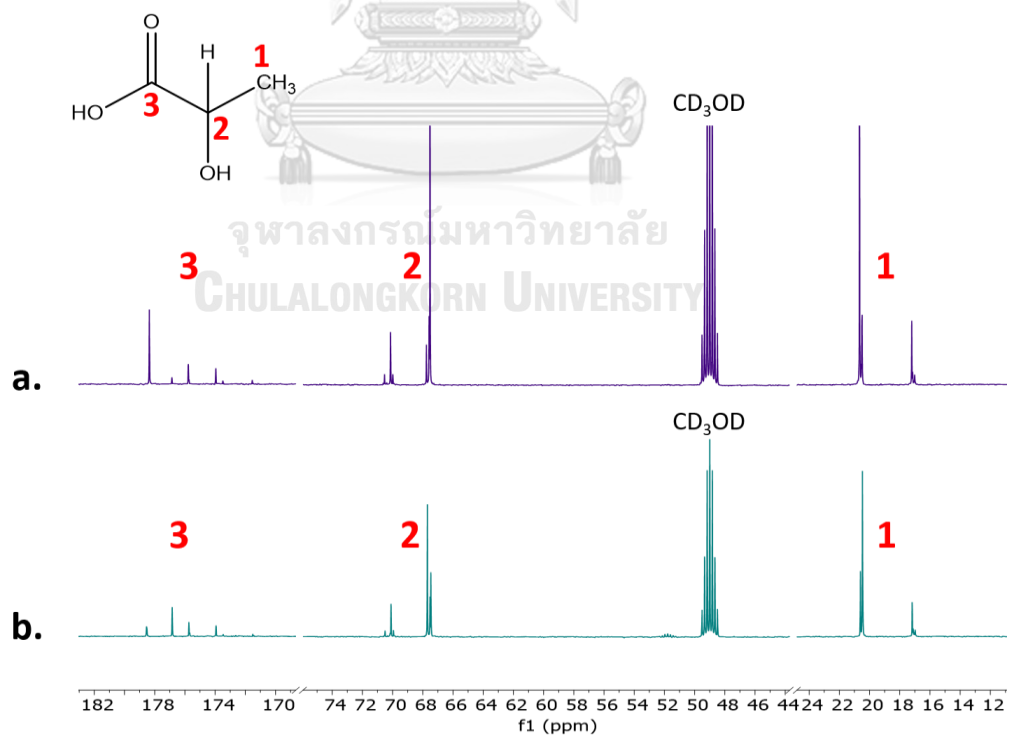
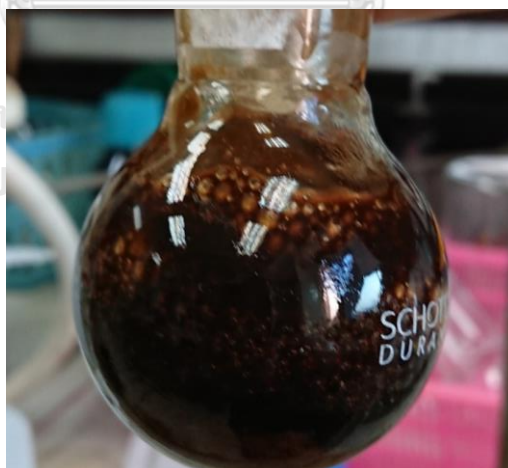


Figure 29.  $^{13}\text{C}$  NMR spectra of a. lactic acid and b. ZnCl<sub>2</sub>-LA DES in CD<sub>3</sub>OD.

$^{13}\text{C}$  NMR spectra of lactic acid (Figure 29a.) showed  $\text{CH}_3$ ,  $\text{CHOH}$ , and  $\text{C}=\text{O}$  signals at  $\delta_{\text{C}}$  20.65, 67.52, and 178.37 ppm, respectively. Compared to lactic acid,  $\text{CH}_3$  and  $\text{CH}$  signals of  $\text{ZnCl}_2$ -LA DES (Figure 29b.) were upfield-shifted, while the signal of  $\text{C}=\text{O}$  was downfield-shifted. In the presence of  $\text{ZnCl}_2$ , the downfield-shifted signal of  $\text{C}=\text{O}$  revealed that  $\text{Zn}^{2+}$  was bonded to  $\text{C}=\text{O}$  and led to the withdrawn electron density. Thus, we proposed that  $\text{Zn}^{2+}$  ions should interact with carboxyl groups of lactic acid as described by Reinoso et al [23].

#### 4.3 Preparation of neat lactic acid pretreated fibres

The neat lactic pretreated fibre was prepared for comparison with  $\text{ZnCl}_2$ -LA DES pretreated fibres. To demonstrate the superior performance of  $\text{ZnCl}_2$ -LA DES compared to the lactic pretreatment, we had chosen our harshest condition for neat lactic acid pretreatment. At the temperature of  $120\text{ }^\circ\text{C}$  for 120 min, the bagasse pulp was dissociated and broken into smaller particles. In Figure 30, the appearance of the solution after 120 min is dark brown and highly viscous, indicating that dehydration of saccharides has occurred in the reaction due to high temperature, acidity, and reaction duration.



**Figure 30.** The visual representation of the bagasse mixture treated with lactic acid after a 120-minute reaction period.

In addition, we had conducted several observations of fibers through a polarized-light microscope after the fabrication of micro- and nanofiber with an ultrasonic homogenizer, and the results were shown the neat lactic acid pretreatment offered an obviously large particle size due to insufficient hydrolysis reaction (Figure 31).

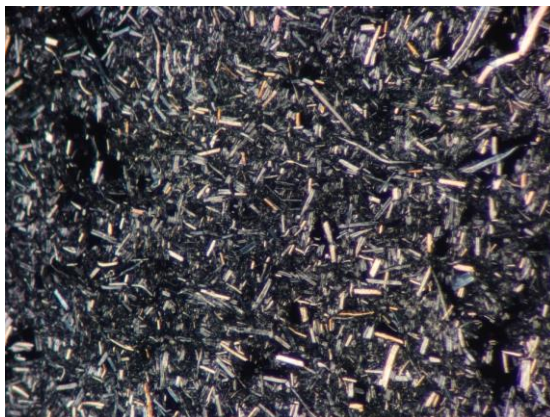


Figure 31. PLM image of lactic acid pretreated bagasse fibre after fabrication with ultrasonic homogenizer.

#### 4.4 Fabrication of CMNFs

##### 4.2.1. Morphology of fibres

In our study on preparation of micro- and nano-cellulose fibers (CMNFs), SCB pulp was treated with zinc chloride- lactic acid deep eutectic solvent and ultrasonication of the fibers in water ( $\text{ZnCl}_2$ -LA/ultrasonication). In treatment with  $\text{ZnCl}_2$ -LA DES, the SCB pulp could be used up to 6.25% of solid loading. Under polarized light microscope, SCB pulp was appeared as tangled long fibers together with bundles of long fibers (Figure 1a). In Figure 32, the  $\text{ZnCl}_2$ -LA DES treated fibers were slightly decreased in length after 180 min of treatment at 60 °C. Fiber length was significantly decreased after treatment at 90 °C for 60 to 180 min and the DES treatment at 90 °C for 180 min resulted in disintegration into short fiber and some of the short fibers had the same width as SCB pulp. The fibers obtained from the 100°C and 110°C treatments exhibited similarity to the fibers obtained from the 90°C treatment, albeit with an increased quantity of smaller fragments as the temperature increased. It was obvious that no large fiber has appeared after treatment at 110 °C for 180 min. At 120 °C of the treatment, we observed fast disintegration of the SCB pulp. Within 30 min, the obtained fibers

were similar to the fibers from treatment at 100 °C for 120 min. However, the DES treatment at 120 °C for longer time resulted in darker color and increased viscosity of the fiber suspension. The fibers obtained from the treatment at 120 °C for 120 min gave a viscous slightly brown suspension which was difficult to filter out and gave the brown fibers after filtration. The appearance of fiber after treatment at 120 °C for 30 and 60 minutes was similar to the fibers obtained after treatment at 110 °C for 120 and 180 minutes respectively.

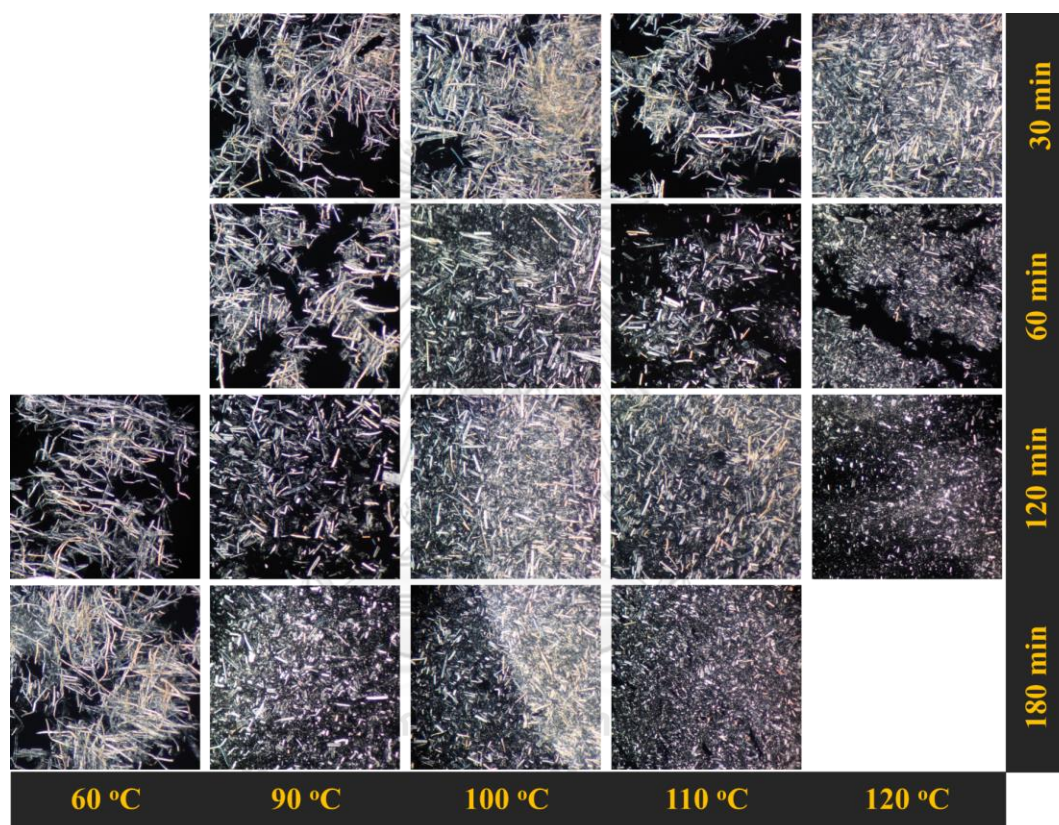
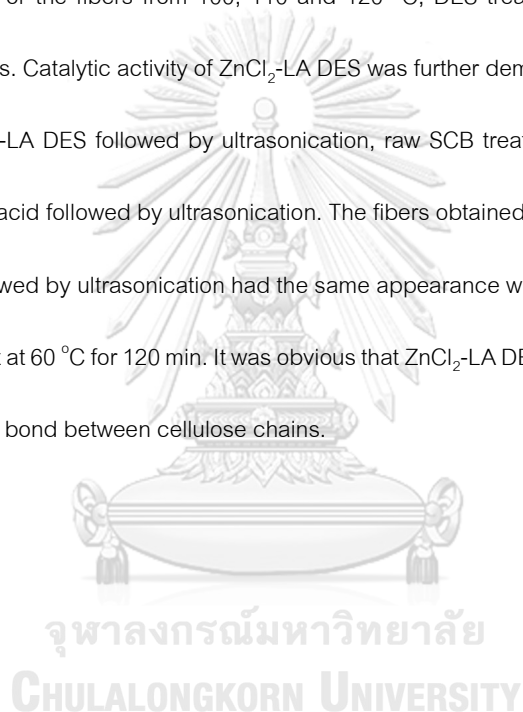


Figure 32. PLM images of DES treated SCB pulp swollen in DI water.

Water suspension of each DES treated fibers in water was then subjected to ultrasonication and the disintegrated fibers were visualized under PLM. After ultrasonication, PLM images of fibers (Figure 33) showed the great performance on disintegration of cellulose fibers. Bundles of the fibers were much more disintegrated to give smaller cylindrical shape fibers with shorter length. Also, the large fragment of fibers was significantly disintegrated by the increased temperature and reaction time. After the ultrasonication, the fibers of each DES-

treated fibers were also well suspended. For the fibers from the 60 °C treatment followed by ultrasonication, the suspension was settled to the bottom of container within less than 1 h while the ultrasonicated suspensions of the 90 and 100 °C DES treated fibers were settled within 24 and 72 h, respectively. These phenomena indicated that the hydrogen bonding between cellulose chains was broken down by assistance of ultrasonication [35] and the cellulose chain could be rebounded after cease of ultrasonication. Among the ultrasonicated suspension, the gel-like suspensions with better translucency were obtained by using 110 and 120 °C treated fibers. For the fibers from 100, 110 and 120 °C, DES treatment followed by ultrasonication resulted in uniform fibers. Catalytic activity of ZnCl<sub>2</sub>-LA DES was further demonstrated by comparing between SCB treated with ZnCl<sub>2</sub>-LA DES followed by ultrasonication, raw SCB treated with ultrasonication, and SCB treated with neat lactic acid followed by ultrasonication. The fibers obtained from neat lactic acid treatment at 120 °C for 120 min followed by ultrasonication had the same appearance with the disintegrated fiber from the ZnCl<sub>2</sub>-LA DES treatment at 60 °C for 120 min. It was obvious that ZnCl<sub>2</sub>-LA DES was very effective on hydrolysis and breaking hydrogen bond between cellulose chains.





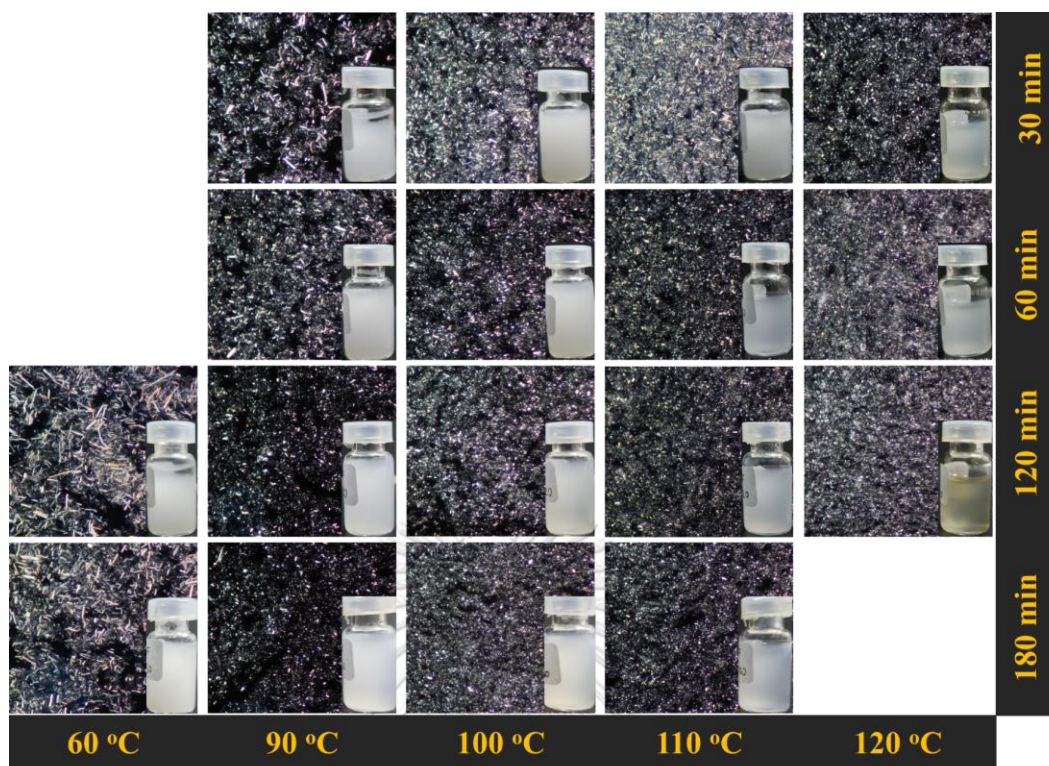


Figure 33. PLM images of CMNF fibers obtained by treatment of the DES treated SCB in water with ultrasonication for 10 minutes.

#### 4.2.2. Particles size

After ultrasonication, the sizes of CMNFs were measured by dynamic light scattering (DLS) and results were presented in Table 3. Ultrasonication of the fibers obtained from mild conditions of DES treatment (Table 3, Entry 1-4 and 7) resulted in cellulose micro- and nanofibers (CMNFs) with the average size over 10,000 nm and most of fibers were clumped together and settled to the bottom of vial within 1 h. For the DES treated fibers from conditions (Entry 5-6, and 8-17, in Table 3), the average size of cellulose nanofibers (CNFs) obtained after ultrasonication was in the range of 332 to 589 nm. The results in Figure 33 and Table 3 also indicated that disintegration with assistance of ultrasonication was significantly increased when small sizes of SCB pulp fibers, provided by DES treatment, were used. In contrast, the ultrasonication of the SCB pulp (large size of the fibers) gave no change of the fiber size. However, the disintegration was declined when the hydrodynamic size of fibers was less than 500 nm. Additionally, increase of the DES treatment time resulted in improvement

of homogeneity of CNFs before and after ultrasonication. TEM images (Figure 34) of the selected conditions showed that CNFs were rod-shaped crystalline cluster with less than 300 nm length and 15-16 nm width (Table 4). CNFs, produced from the 90 °C ZnCl<sub>2</sub>-LA DES treatment/ultrasonication, were packed together to give long bundles of the crystalline fibers with the fiber bundle dimension of >1000 nm length and 80 nm width (Figure 34a). When the fibers from the DES treatment at  $\geq 100$  °C was further disintegrated by ultrasonication, the fiber bundles were obtained as smaller clusters of crystalline fibers (Figure 34b-d). The results also proved that temperature and time of ZnCl<sub>2</sub>-LA DES treatment and ultrasonication were crucial factors in acceleration of fiber disintegration. At high temperature, a presence of ZnCl<sub>2</sub> as Lewis acid however resulted in dark color by-products [3]. Furthermore, TEM of the fibers from 120 °C DES treatment/ultrasonication revealed a presence of unknown polymer (Figure 34d., in red circle) holding the fiber which might cause increase of fibers size in dynamic light scattering (DLS) analysis.

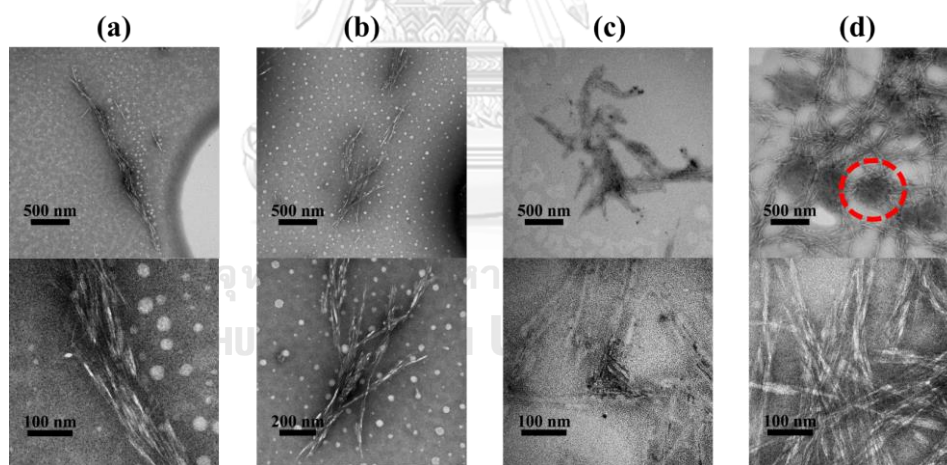


Figure 34. TEM images of CMNF from different temperatures at: (a) 90 °C, (b) 100 °C, (c) 110 °C, and (d) 120 °C for 120 min.



**Table 3.** DLS results of CMNFs from different reaction temperatures and times.

Entry	Label <sup>a</sup>	Reaction temp (°C)	Reaction time (min)	Hydrodynamic size <sup>b</sup> (nm)
1	60_120	60	120	>10,000 <sup>c</sup>
2	60_180	60	180	>10,000 <sup>c</sup>
3	90_30	90	30	>10,000 <sup>c</sup>
4	90_60	90	60	>10,000 <sup>c</sup>
5	90_120	90	120	452
6	90_180	90	180	370
7	100_30	100	30	>10,000 <sup>c</sup>
8	100_60	100	60	518
9	100_120	100	120	463
10	100_180	100	180	361
11	110_30	110	30	345
12	110_60	110	60	359
13	110_120	110	120	305
14	110_180	110	180	365
15	120_30	120	30	340
16	120_60	120	60	320
17	120_120	120	120	512

<sup>a</sup>Labels were represented reactions temperature and time, respectively.

<sup>b</sup>Hydrodynamic sizes were calculated by DLS particle size analyzer. <sup>c</sup>Sizes were larger than analysis range of machine (>10,000 nm).

**Table 4.** CMNF dimensions and Crl from different temperature.

Entry	Reaction temp (°C)	Reaction time (min)	Length <sup>a</sup> (nm)	Width <sup>a</sup> (nm)
1	90	120	259 ± 33	15 ± 4
2	100	120	236 ± 35	15 ± 4
3	110	120	-	-
4	120	120	279 ± 33	16 ± 7

<sup>a</sup>Length and width of CMNFs were measured with ImageJ based on TEM images.

#### 4.2.3. Characteristics of fibres

FTIR spectra of SCB pulp and CMNFs (Figure 35) were showed characteristics of cellulose with absorption at 3332 cm<sup>-1</sup> (O—H stretching vibration), 2893 cm<sup>-1</sup> (C—H stretching), 1645 cm<sup>-1</sup> (water-absorbed fibers and carboxylates from bleaching process), 1430 cm<sup>-1</sup> (characteristic C—H deformation vibration of cellulose I), 1370 cm<sup>-1</sup> (C—H bending vibration), 1160 cm<sup>-1</sup> (C—O—C stretching vibration), 1052 cm<sup>-1</sup> (ring stretching

vibration), and  $896\text{ cm}^{-1}$  (C—H deformation vibration) [50]. In Figure 35b and 35c a stretching vibration of C=O at  $1737\text{ cm}^{-1}$  and small shoulder at  $2880\text{ cm}^{-1}$  and  $2910\text{ cm}^{-1}$  for CH—OH and  $\text{CH}_3$  stretching indicated a presence of lactate ester. When the reaction temperature reached  $120\text{ }^\circ\text{C}$ , a broad absorption at  $1596\text{ cm}^{-1}$  indicated a presence of C=C conjugated structure (Figure 35b). Due to an absence of aromatic group in the SCB pulp spectrum, the conjugated structure should be arisen from degradation of cellulose molecule through dehydration of glucose at temperature above  $120\text{ }^\circ\text{C}$  [3]. In Figure 35b and 35c, a stretching vibration of C=O at  $1737\text{ cm}^{-1}$  and small shoulder at  $2880\text{ cm}^{-1}$  and  $2910\text{ cm}^{-1}$  for C-H stretching vibration of CH—OH and  $\text{CH}_3$  indicated a presence of lactate ester.

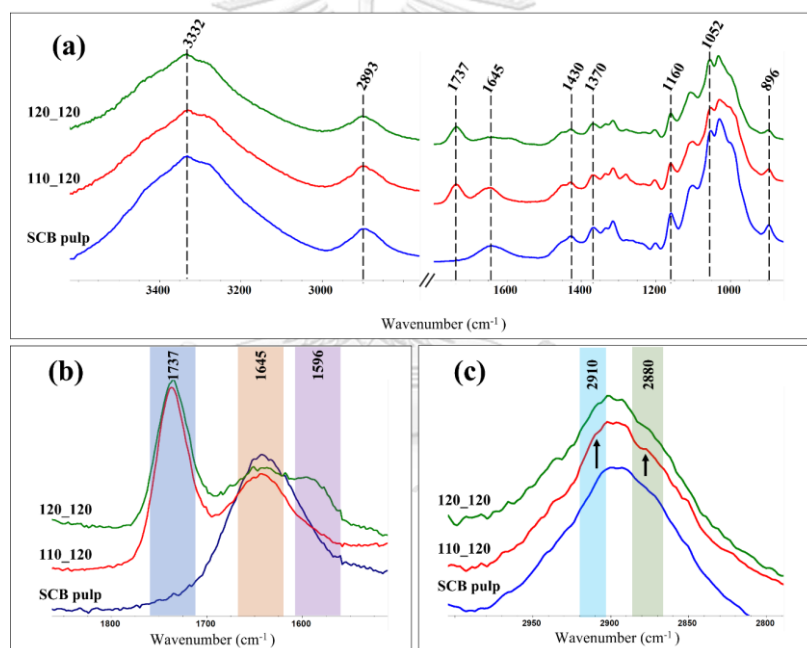


**Figure 35.** (a) FTIR spectra of bleached SCB pulp and CMNF samples from different temperature, (b) and (c) Cropped FTIR spectra.

On basis of solid-state NMR analysis,  $^{13}\text{C}$  spectrum of the fibers from  $110\text{ }^\circ\text{C}$  (120min) DES treatment/ultrasonication (Figure 36) showed common signals of cellulose at  $\delta_{\text{C}}$  62.6 ppm (C-6, amorphous cellulose), 64.9 ppm (C-6, crystalline cellulose), 72-75 ppm (C-2,3,5), 84.1 ppm (C-4, amorphous cellulose), 88.6 ppm (C-4, crystalline cellulose), and 104.9 ppm (C-1) [20], and additional signals of methyl and carbonyl

carbons for lactate ester at  $\delta_c$  20 and 175 ppm, respectively [20]. Thus it was confirmed that lactate ester was occurred during  $ZnCl_2$ -LA DES treatment.

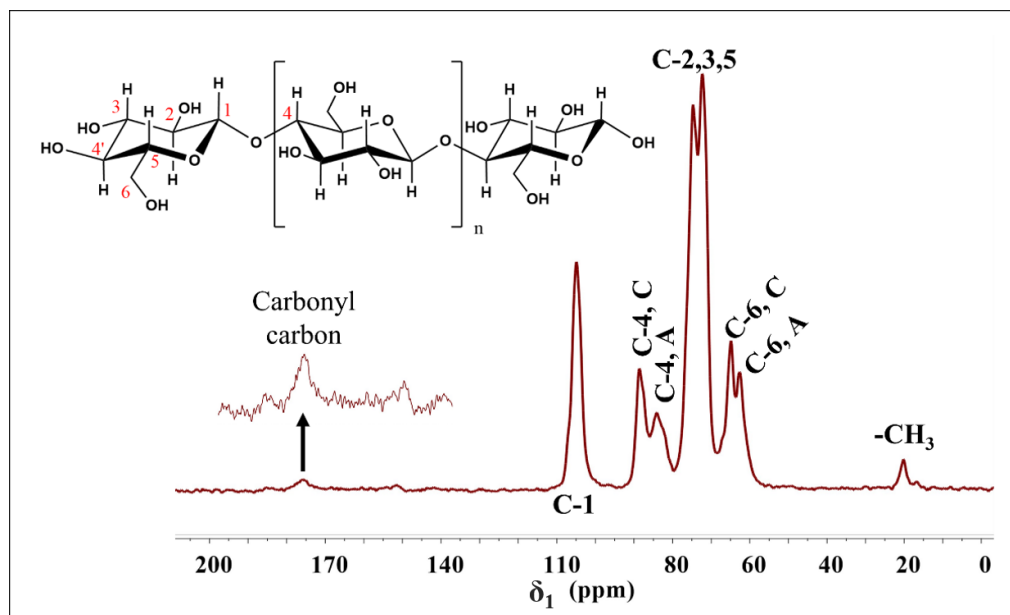


Figure 36.  $^{13}C$  solid-state NMR of CMNF obtained from  $ZnCl_2$ -LA DES treated CMNF.

The XRD results of the CMNFs (Figure 37) showed the diffraction peaks at  $2\theta = 14.9, 16.0, 22.4,$  and  $34.7^\circ$  corresponding to cellulose crystal plane (1-10), (110), (200), and (004) respectively[49]. For fibers treated with  $ZnCl_2$ -LA DES at  $110^\circ C$  for 2 h followed by ultrasonication (Table 5, Entry 3), the crystallinity of CMNF was reached 62.2%. Based on the absorption of the conjugated structure in the FTIR spectrum of the CMNF obtained from treatment with  $ZnCl_2$ -LA DES at  $120^\circ C$  for 120 min, followed by ultrasonication, the reduction of CrI to 55% may have been caused by the catalytic decomposition of crystalline cellulose [21].

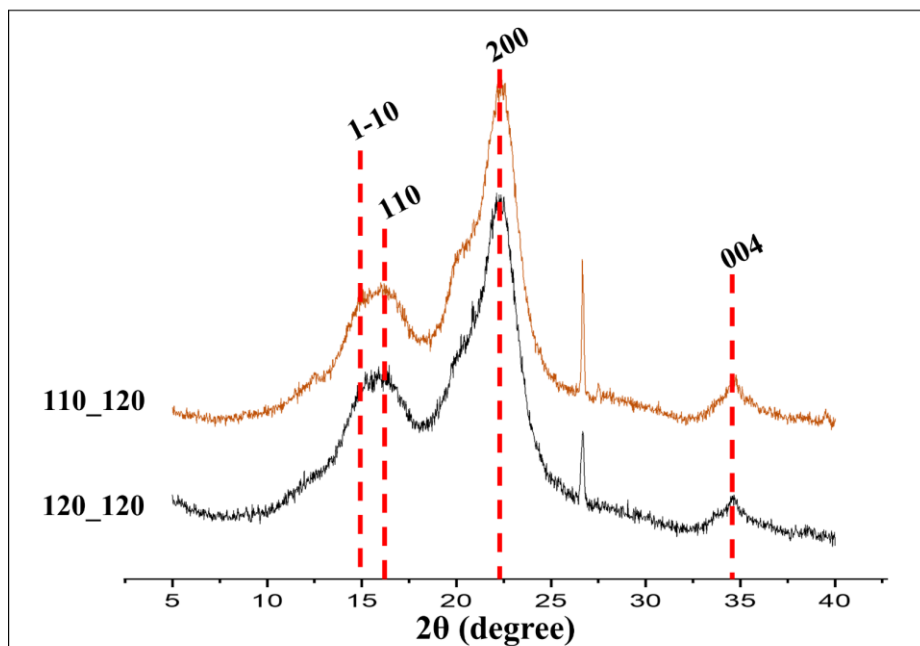


Figure 37. XRD results of obtained CMNF.

Table 5. CMNF dimensions and CrI from different temperature

Entry	Reaction temp (°C)	Reaction time (min)	Yield (%) <sup>b</sup>	CrI (%) <sup>c</sup>
1	90	120	95	59.4
2	100	120	94	59.7
3	110	120	94	62.2
4	120	120	67	55.1

<sup>a</sup>Length and width of CMNFs were measured with ImageJ based on TEM images.

<sup>b</sup>Yield of CMNFs were calculated from dry mass of SCB pulp and ZnCl<sub>2</sub>-LA DES treated fibers. <sup>c</sup>CrI of CMNFs were calculated from XRD data.

In literatures, ZnCl<sub>2</sub>-cellulose complex obtained from zinc chloride ionic liquid led to large reduction of crystallinity (from 47% to 20%) because the crystalline core of cellulose fibers could be destroyed by dissolution mechanism [20, 26, 36]. In contrast, our work revealed that ZnCl<sub>2</sub>-LA DES increased the crystallinity of fibers. Since the dissolution of cellulose crystalline structure was prevented by functionalized cellulose [50], the lactate functionalized cellulose in our work might result in the improvement of the hydrophobicity of cellulose high CrI.

#### 4.2.4. Mechanism

In literatures, many works proposed that  $\text{ZnCl}_2$  was changed into zinc chloride hexahydrate complex ( $[\text{Zn}(\text{H}_2\text{O})_6][\text{ZnCl}_4]$ ) when it became ionic liquid and the complex formed stable hydrogen bond between cellulose chain [21, 26, 28, 36, 38]. The  $\text{ZnCl}_2$ -cellulose complex obtained from those zinc chloride ionic liquid led to large reduction of crystallinity (from 47% to 20%) because the crystalline core of cellulose fibers could be destroyed by dissolution mechanism [21, 26, 36]. In contrast, our work revealed that  $\text{ZnCl}_2$ -LA DES increased the crystallinity of fibers. Thus, the reaction mechanism of  $\text{ZnCl}_2$ -LA DES and zinc chloride ionic liquids should be different. Since the dissolution of cellulose crystalline structure was prevented by functionalized cellulose [50], the lactate functionalized cellulose in our work might resulted in improvement of the hydrophobicity of cellulose and the CNFs with high CrI was then obtained. From the  $^1\text{H}$  and  $^{13}\text{C}$  NMR analysis, we proposed that  $\text{Zn}^{2+}$  ions should interact with carboxyl groups of lactic acid as described by Reinoso et al [23]. On basis of NMR analysis and previous reports, we proposed mechanism of cellulose hydrolysis and LA-functionalization in  $\text{ZnCl}_2$ -LA DES as shown in Figure 38.

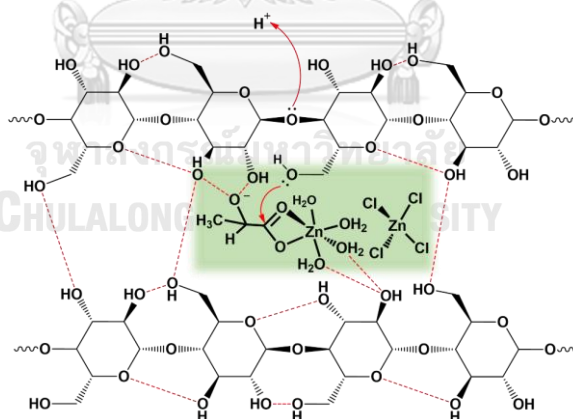


Figure 38. Possible mechanism of cellulose chain cleavage and functionalized in  $\text{ZnCl}_2$ -LA DES.

#### 4.5 Preparation of CMNF films

As mentioned above, increased of time for DES treatment resulted in higher uniform fibers. Thus, cellulose films from the CMNFs were prepared by vacuum filtration method to give translucent films as shown in Figure 39. The translucency of films was increased by size and uniformity of the CMNFs. The uniform CNFs with 332 nm of average size, obtained by 110 °C (120 min) ZnCl<sub>2</sub>-LA DES treatment/ultrasonication, provided a tough film with higher translucency, while the film from CMNFs with >500 nm of average size was softer.



Figure 39. Cellulose films obtained from fibers treated with ZnCl<sub>2</sub>-LA at 110 °C for: (a) 30 minutes and (b) 120 minutes

#### 4.6 Reusing of ZnCl<sub>2</sub>-LA DES

##### 4.2.1. Reuse of ZnCl<sub>2</sub>-LA DES

In DES treatment process, color of the used ZnCl<sub>2</sub>-LA DES from each condition (Figure 40) was darker by increase of temperature and time of the treatment. When suspension of the DES-treated fibers was brown, the treated fibers were filtered out and the DES was directly reused in DES treatment process. The brown DES resulted in brown to dark fibers due to by-products in the used DES. It was found that color of the used DES and these unwanted by-products could be eliminated by dilution with water and decolorization with activated carbon. Then the colorless clear DES solution in water was evaporated *in vacuo* and subjected to <sup>1</sup>H and <sup>13</sup>C NMR analysis. The NMR results of the decolorized DES were similar to the freshly prepared ZnCl<sub>2</sub>-LA DES.

When the decolorized DES was evaluated in the 110 °C (120 min) DES treatment process, it could be reused up to 5 times and gave the fibers with average size from 364 to 387 nanometers in >90% yield (Table 6).



Figure 40. Images of used solvent from different temperatures and reaction times.

Table 6. Yield and CMNF sizes reply to ZnCl<sub>2</sub>-LA DES reusing times.

Reused number (times)	Hydrodynamic size (nm)	Yield (%)	CrI (%)
0	332 ± 157	94	62.2
1	364 ± 169	94	n/a
2	377 ± 106	94	n/a
3	373 ± 99	94	n/a
4	366 ± 139	96	59.2
5	387 ± 92	98	59.6



Figure 41. PLM images of CMNF fibers obtained by SCB pretreated with reuse DES.

#### 4.2.2. NMR analysis

After four cycles use of  $\text{ZnCl}_2$ -LA DES, the  $\text{CH}_3$  and CH signals were slightly downfield-shifted and upfield-shifted, respectively, and the reused DES contained less amount of lactic acid oligomers when compared to fresh  $\text{ZnCl}_2$ -LA DES. In addition of small amount of  $\text{ZnCl}_2$  into the reused  $\text{ZnCl}_2$ -LA DES,  $^1\text{H}$  NMR result showed that  $\delta_{\text{H}}$  of the  $\text{CH}_3$  and CH were similar to the freshly prepared  $\text{ZnCl}_2$ -LA DES. Although, these results revealed a few losses of  $\text{ZnCl}_2$  in each cycle of the DES treatment, the  $\text{ZnCl}_2$ -LA DES could be reused up to 5 cycles.



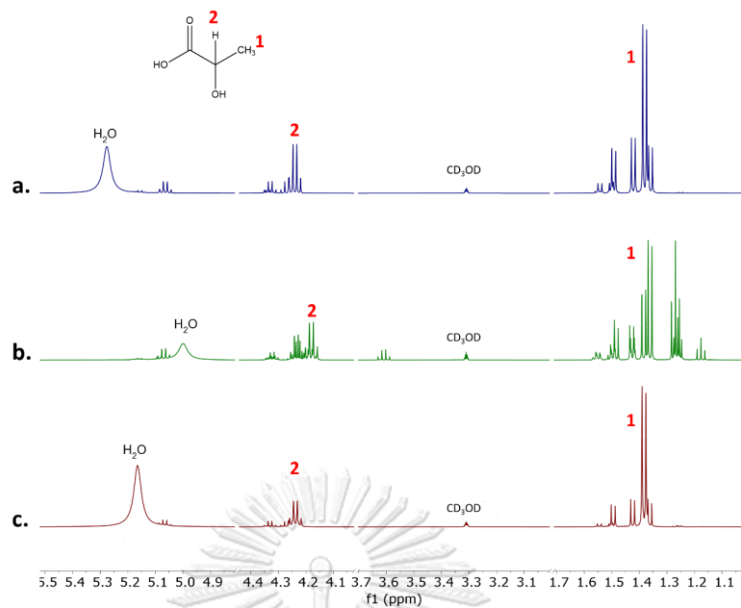


Figure 42.  $^1\text{H}$  NMR spectra in  $\text{CD}_3\text{OD}$  of  $\text{ZnCl}_2$ -LA DES, used  $\text{ZnCl}_2$ -LA DES, reuse  $\text{ZnCl}_2$ -LA DES.

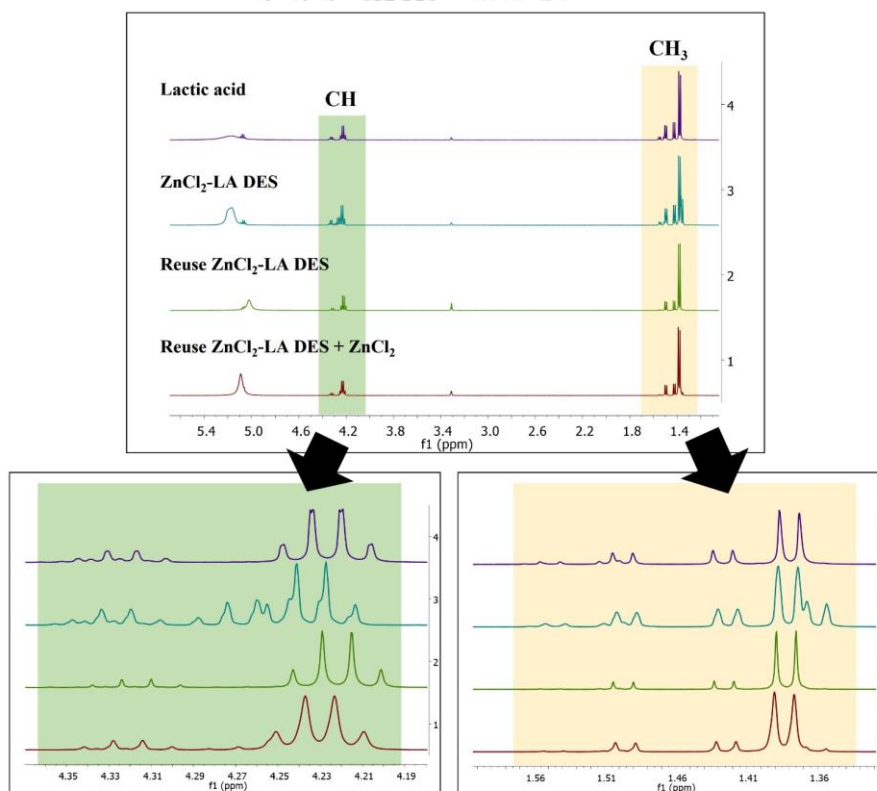


Figure 43.  $^1\text{H}$  NMR spectra in  $\text{CD}_3\text{OD}$  of lactic acid,  $\text{ZnCl}_2$ -LA DES, reuse  $\text{ZnCl}_2$ -LA DES (reuse 3rd time), and reuse  $\text{ZnCl}_2$ -LA DES (reuse 3rd time) with  $\text{ZnCl}_2$  added.

#### 4.7 Recover of zinc

To maintain the consistency of  $\text{ZnCl}_2$ -LA DES performance, the number of reuses must be limited. The used solvent was then terminated and went to recycling process. The recycling process was done by precipitation of zinc chloride from solution as a water-insoluble salt by added oxalic acid solution and left just saccharides and derivatives in solution, the white precipitate of zinc oxalate was then filtered out and then calcined to retrieved zinc oxide which is precursor of zinc chloride (Figure 44).

The obtained zinc oxalate powder was subjected to XRD analysis. The XRD spectra of our zinc oxalate sample was perfectly match to JCPDS card no. 251029 for zinc oxalate dehydrated[51] (Figure 45.).



Figure 44. zinc oxalate powder obtained by precipitation from used DES.

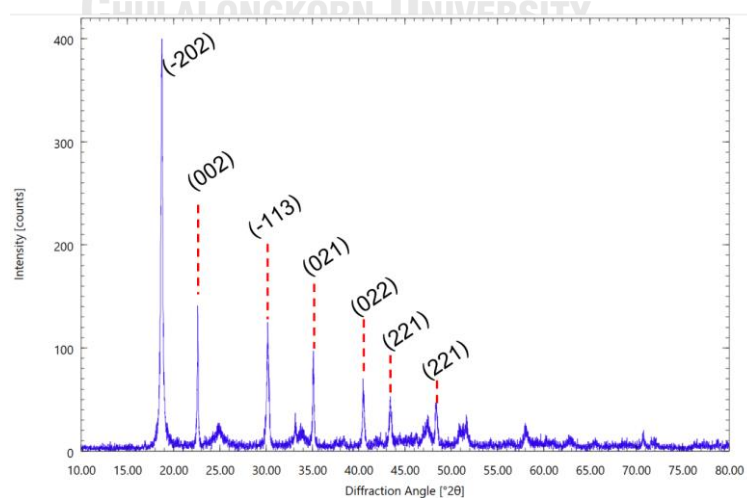


Figure 45. XRD spectra of obtained zinc oxalate.

## CHAPTER V

### CONCLUSION

#### 5.1. Conclusion

Green and reliable  $\text{ZnCl}_2$ -LA DES was deployed in SCB pulp treatment to preparing of CMNFs. The obtained fibers after separated by very fast ultrasonication had yield more than 90% and improved the crystallinity up to 62.2% with average width 15-16 nm and 236-279 nm long. The  $\text{ZnCl}_2$ -LA DES treatment consumed less energy and used short treatment time than neat lactic acid treatment and reduce the ultrasonication time compared to previous studies.  $\text{ZnCl}_2$ -LA DES can be used up to 5 cycles and more, the obtained fibers from 5<sup>th</sup> cycle had 98% yield and CrI equal 59.6% the average size was 387 nm compared to 305 nm obtained from fresh prepared solvent. Zinc ion in  $\text{ZnCl}_2$ -LA DES can be recovered with easy and low environment impact procedure, recovered zinc compounds were easy to be isolated with high purity and used to converted back to zinc chloride again. From achieved results, the  $\text{ZnCl}_2$ -LA DES had high efficiency for cellulose micro- and nanofibers separation from bleached SCB pulp, ability to reuse up to 5 times, and can be recycled. The treatment bleached SCB pulp with novel DES and very fast ultrasonic nanofibrillation were proved to be a sustainable method to obtained high yield and high quality CMNF from biomass.

## REFERENCES

- [1] S. Sankhla, H.H. Sardar, S. Neogi, Greener extraction of highly crystalline and thermally stable cellulose micro-fibers from sugarcane bagasse for cellulose nano-fibrils preparation, *Carbohydr. Polym.*, 251 (2021) 117030.
- [2] F.V. Ferreira, M. Mariano, S.C. Rabelo, R.F. Gouveia, L.M.F. Lona, Isolation and surface modification of cellulose nanocrystals from sugarcane bagasse waste: From a micro- to a nano-scale view, *Appl. Surf. Sci.*, 436 (2018) 1113-1122.
- [3] Q. Ji, X. Yu, A.E.-G.A. Yagoub, L. Chen, C. Zhou, Efficient cleavage of strong hydrogen bonds in sugarcane bagasse by ternary acidic deep eutectic solvent and ultrasonication to facile fabrication of cellulose nanofibers, *Cellulose*, 28 (2021) 6159-6182.
- [4] A. Barhoum, J. Jeevanandam, A. Rastogi, P. Samyn, Y. Boluk, A. Dufresne, M.K. Danquah, M. Bechelany, Plant celluloses, hemicelluloses, lignins, and volatile oils for the synthesis of nanoparticles and nanostructured materials, *Nanoscale*, 12 (2020) 22845-22890.
- [5] G.J.M. Rocha, A.R. Gonçalves, B.R. Oliveira, E.G. Olivares, C.E.V. Rossell, Steam explosion pretreatment reproduction and alkaline delignification reactions performed on a pilot scale with sugarcane bagasse for bioethanol production, *Ind. Crops Prod.*, 35 (2012) 274-279.
- [6] S. Zhang, J. Sun, X. Zhang, J. Xin, Q. Miao, J. Wang, Ionic liquid-based green processes for energy production, *Chem. Soc. Rev.*, 43 (2014) 7838-7869.
- [7] J.S. Mahajan, R.M. O'Dea, J.B. Norris, L.T.J. Korley, T.H. Epps, III, Aromatics from lignocellulosic biomass: A platform for high-performance thermosets, *ACS Sustain. Chem. Eng.*, 8 (2020) 15072-15096.
- [8] N.N. Antonio, Y. Hiroyuki, Cellulose-Nanofiber-Based Materials, in: J. Hinestroza, A.N. Netravali (Eds.) *Cellulose Based Composites: New Green Nanomaterials*, Wiley-Vch Verlag, Germany, 2014, pp. 3-22.
- [9] V. Thakur, A. Guleria, S. Kumar, S. Sharma, K. Singh, Recent advances in nanocellulose processing, functionalization and applications: a review, *Mater. Adv.*, 2 (2021) 1872-1895.

- [10] X. Wang, Z. Pang, C. Chen, Q. Xia, Y. Zhou, S. Jing, R. Wang, U. Ray, W. Gan, C. Li, G. Chen, B. Foster, T. Li, L. Hu, All-natural, degradable, rolled-up straws based on cellulose micro- and nano-hybrid fibers, *Adv. Funct. Mater.*, 30 (2020) 1910417.
- [11] A. Farooq, M.K. Patoary, M. Zhang, H. Mussana, M. Li, M.A. Naeem, M. Mushtaq, A. Farooq, L. Liu, Cellulose from sources to nanocellulose and an overview of synthesis and properties of nanocellulose/zinc oxide nanocomposite materials, *Int. J. Biol. Macromol.*, 154 (2020) 1050-1073.
- [12] D. Trache, A.F. Tarchoun, M. Derradji, T.S. Hamidon, N. Masruchin, N. Brosse, M.H. Hussin, Nanocellulose: From fundamentals to advanced applications, *Front. Chem.*, 8 (2020) 392.
- [13] T.J. Bondancia, J. de Aguiar, G. Batista, A.J.G. Cruz, J.M. Marconcini, L.H.C. Mattoso, C.S. Farinas, Production of nanocellulose using citric acid in a biorefinery concept: Effect of the hydrolysis reaction time and techno-economic analysis, *Ind. Eng. Chem. Res.*, 59 (2020) 11505-11516.
- [14] Y. Chen, T. Mu, Application of deep eutectic solvents in biomass pretreatment and conversion, *Green energy environ.*, 4 (2019) 95-115.
- [15] H. Wang, H. Xie, H. Du, X. Wang, W. Liu, Y. Duan, X. Zhang, L. Sun, X. Zhang, C. Si, Highly efficient preparation of functional and thermostable cellulose nanocrystals via H<sub>2</sub>SO<sub>4</sub> intensified acetic acid hydrolysis, *Carbohydr. Polym.*, 239 (2020) 116233.
- [16] S. Salimi, R. Sotudeh-Gharebagh, R. Zarghami, S.Y. Chan, K.H. Yuen, Production of nanocellulose and its applications in drug delivery: A critical review, *ACS Sustain. Chem. Eng.*, 7 (2019) 15800-15827.
- [17] I. Bodachivskyi, U. Kuzhiumparambil, D.B.G. Williams, Catalytic valorization of native biomass in a deep eutectic solvent: A systematic approach toward high-yielding reactions of polysaccharides, *ACS Sustain. Chem. Eng.*, 8 (2020) 678-685.
- [18] Z. Chen, X. Bai, Lusi, C. Wan, High-solid lignocellulose processing enabled by natural deep eutectic solvent for lignin extraction and industrially relevant production of renewable chemicals, *ACS Sustain. Chem. Eng.*, 6 (2018) 12205-12216.

- [19] S. Hong, H. Lian, X. Sun, D. Pan, A. Carranza, J.A. Pojman, J.D. Mota-Morales, Zinc-based deep eutectic solvent-mediated hydroxylation and demethoxylation of lignin for the production of wood adhesive, *RSC Adv.*, 6 (2016) 89599-89608.
- [20] J. Jiang, N.C. Carrillo-Enríquez, H. Oguzlu, X. Han, R. Bi, J.N. Saddler, R.-C. Sun, F. Jiang, Acidic deep eutectic solvent assisted isolation of lignin containing nanocellulose from thermomechanical pulp, *Carbohydr. Polym.*, 247 (2020) 116727.
- [21] J. Jiang, N.C. Carrillo-Enríquez, H. Oguzlu, X. Han, R. Bi, M. Song, J.N. Saddler, R.-C. Sun, F. Jiang, High production yield and more thermally stable lignin-containing cellulose nanocrystals isolated using a ternary acidic deep eutectic solvent, *ACS Sustain. Chem. Eng.*, 8 (2020) 7182-7191.
- [22] P. Kalhor, K. Ghandi, Deep eutectic solvents for pretreatment, extraction, and catalysis of biomass and food waste, *Molecules*, 24 (2019) 4012.
- [23] P. Li, J.A. Sirviö, A. Haapala, H. Liimatainen, Cellulose nanofibrils from nonderivatizing urea-based deep eutectic solvent pretreatments, *ACS Appl. Mater. Interfaces*, 9 (2017) 2846-2855.
- [24] X. Li, H. Li, T. You, X. Chen, S. Ramaswamy, Y.-Y. Wu, F. Xu, Enhanced dissolution of cotton cellulose in 1-allyl-3-methylimidazolium chloride by the addition of metal chlorides, *ACS Sustain. Chem. Eng.*, 7 (2019) 19176-19184.
- [25] Q. Liu, T. Yuan, Q.-J. Fu, Y.-Y. Bai, F. Peng, C.-L. Yao, Choline chloride-lactic acid deep eutectic solvent for delignification and nanocellulose production of moso bamboo, *Cellulose*, 26 (2019) 9447-9462.
- [26] S. Liu, Q. Zhang, S. Gou, L. Zhang, Z. Wang, Esterification of cellulose using carboxylic acid-based deep eutectic solvents to produce high-yield cellulose nanofibers, *Carbohydr. Polym.*, 251 (2021) 117018.
- [27] Y. Liu, W. Chen, Q. Xia, B. Guo, Q. Wang, S. Liu, Y. Liu, J. Li, H. Yu, Efficient cleavage of lignin-carbohydrate complexes and ultrafast extraction of lignin oligomers from wood biomass by microwave-assisted treatment with deep eutectic solvent, *ChemSusChem*, 10 (2017) 1692-1700.
- [28] Y.-L. Loow, T.Y. Wu, G.H. Yang, L.Y. Ang, E.K. New, L.F. Siow, J. Md Jahim, A.W. Mohammad, W.H. Teoh, Deep eutectic solvent and inorganic salt pretreatment of

- lignocellulosic biomass for improving xylose recovery, *Bioresour. Technol.*, 249 (2018) 818-825.
- [29] Y. Ma, Q. Xia, Y. Liu, W. Chen, S. Liu, Q. Wang, Y. Liu, J. Li, H. Yu, Production of nanocellulose using hydrated deep eutectic solvent combined with ultrasonic treatment, *ACS Omega*, 4 (2019) 8539-8547.
- [30] P. Maneechakr, S. Karnjanakom, Catalytic conversion of fructose into 5-HMF under eco-friendly-biphasic process, *React. Chem. Eng.*, 5 (2020) 2058-2063.
- [31] A. Peñaranda Gómez, O. Rodríguez Bejarano, V.V. Kouznetsov, C. Ochoa-Puentes, One-pot diastereoselective synthesis of tetrahydroquinolines from star anise oil in a choline chloride/zinc chloride eutectic mixture, *ACS Sustain. Chem. Eng.*, 7 (2019) 18630-18639.
- [32] A. Satlewal, R. Agrawal, S. Bhagia, J. Sangoro, A.J. Ragauskas, Natural deep eutectic solvents for lignocellulosic biomass pretreatment: Recent developments, challenges and novel opportunities, *Biotechnol. Adv.*, 36 (2018) 2032-2050.
- [33] J.A. Sirviö, Fabrication of regenerated cellulose nanoparticles by mechanical disintegration of cellulose after dissolution and regeneration from a deep eutectic solvent, *J. Mater. Chem. A Mater. Energy Sustain.*, 7 (2019) 755-763.
- [34] J.A. Sirviö, M. Visanko, H. Liimatainen, Acidic deep eutectic solvents as hydrolytic media for cellulose nanocrystal production, *Biomacromolecules*, 17 (2016) 3025-3032.
- [35] E.L. Smith, A.P. Abbott, K.S. Ryder, Deep eutectic solvents (DESs) and their applications, *Chem. Rev.*, 114 (2014) 11060-11082.
- [36] H. Wang, J. Li, X. Zeng, X. Tang, Y. Sun, T. Lei, L. Lin, Extraction of cellulose nanocrystals using a recyclable deep eutectic solvent, *Cellulose*, 27 (2020) 1301-1314.
- [37] Q. Xia, Y. Liu, J. Meng, W. Cheng, W. Chen, S. Liu, Y. Liu, J. Li, H. Yu, Multiple hydrogen bond coordination in three-constituent deep eutectic solvents enhances lignin fractionation from biomass, *Green Chem.*, 20 (2018) 2711-2721.
- [38] X. Yang, H. Xie, H. Du, X. Zhang, Z. Zou, Y. Zou, W. Liu, H. Lan, X. Zhang, C. Si, Facile extraction of thermally stable and dispersible cellulose nanocrystals with high yield via a green and recyclable FeCl<sub>3</sub>-catalyzed deep eutectic solvent system, *ACS Sustain. Chem. Eng.*, 7 (2019) 7200-7208.

- [39] B. Liu, W. Fu, X. Lu, Q. Zhou, S. Zhang, Lewis acid–base synergistic catalysis for polyethylene terephthalate degradation by 1,3-dimethylurea/Zn(OAc)<sub>2</sub> deep eutectic solvent, *ACS Sustain. Chem. Eng.*, 7 (2019) 3292-3300.
- [40] U.N.S. Division, Thailand-Bagasse Production, United Nations, <http://data.un.org/Data.aspx?d=EDATA&f=cmlID%3aBS%3btrID%3a01>, 2020.
- [41] P.J. Harris, PRIMARY AND SECONDARY PLANT CELL WALLS: A COMPARATIVE OVERVIEW\*, 2006.
- [42] P. Chen, Y. Nishiyama, J.-L. Putaux, K. Mazeau, Diversity of potential hydrogen bonds in cellulose I revealed by molecular dynamics simulation, *Cellulose*, 21 (2014) 897-908.
- [43] A. Dufresne, Nanocellulose: From nature to high performance tailored materials, De Gruyter, Berlin, Germany, 2012.
- [44] Y. Zhao, H. Sun, B. Yang, Y. Weng, Hemicellulose-based film: Potential green films for food packaging, *Polymers (Basel)*, 12 (2020) 1775.
- [45] Handbook of Nanocellulose and Cellulose Nanocomposites: 2 Volume Set, Wiley-VCH Verlag, Weinheim, Germany, 2017.
- [46] F. Torres, S. Commeaux, O. Troncoso, Biocompatibility of bacterial cellulose based biomaterials, *J. Funct. Biomater.*, 3 (2012) 864-878.
- [47] Y. Marcus, Deep eutectic solvents, Springer International Publishing, Cham, 2019.
- [48] M. Lara-Serrano, S. Morales-delaRosa, J.M. Campos-Martín, J.L.G. Fierro, High enhancement of the hydrolysis rate of cellulose after pretreatment with inorganic salt hydrates, *Green Chemistry*, 22 (2020) 3860-3866.
- [49] S. Nam, A.D. French, B.D. Condon, M. Concha, Segal crystallinity index revisited by the simulation of X-ray diffraction patterns of cotton cellulose I $\beta$  and cellulose II, *Carbohydr. Polym.*, 135 (2016) 1-9.
- [50] M. Cheng, Z. Qin, Y. Chen, S. Hu, Z. Ren, M. Zhu, Efficient extraction of cellulose nanocrystals through hydrochloric acid hydrolysis catalyzed by inorganic chlorides under hydrothermal conditions, *ACS Sustain. Chem. Eng.*, 5 (2017) 4656-4664.
- [51] E.P. Etape, J. Foba-Tendo, L.J. Ngolui, B.V. Namondo, F.C. Yollande, M.B.N. Nguimezong, Structural Characterization and Magnetic Properties of Undoped and Ti-



Doped ZnO Nanoparticles Prepared by Modified Oxalate Route, Journal of Nanomaterials, 2018 (2018) 9072325.





จุฬาลงกรณ์มหาวิทยาลัย  
**CHULALONGKORN UNIVERSITY**

## VITA

NAME Worapoj Phuckpetch

DATE OF BIRTH 30 October 1994

PLACE OF BIRTH Nopparat Rajathanee Hospital, Bangkok

INSTITUTIONS ATTENDED Chulalongkorn University

HOME ADDRESS 100/257 Village No.2 Sukhumvit Road, Plutaluang Sub-district,  
Sattahip District, Chonburi, 20180

